



Coumarins-lipophilic cations conjugates: Efficient mitocans targeting carbonic anhydrases

Alma Fuentes-Aguilar^{a,b}, Aday González-Bakker^c, Mirna Jovanović^d, Sofija Jovanović Stojanov^d, Adrián Puerta^c, Adriana Gargano^e, Jelena Dinić^d, José L. Vega-Báez^a, Penélope Merino-Montiel^a, Sara Montiel-Smith^a, Stefano Alcaro^{e,f,g}, Alessio Nocentini^h, Milica Pešić^{d,*}, Claudiu T. Supuran^{h,*}, José M. Padrón^{c,*}, José G. Fernández-Bolaños^b, Óscar López^{b,*}

^a Facultad de Ciencias Químicas, Benemérita Universidad Autónoma de Puebla, Ciudad Universitaria, 72570 Puebla, PUE, Mexico

^b Departamento de Química Orgánica, Facultad de Química, Universidad de Sevilla, Apartado 1203, E-41071 Seville, Spain

^c BioLab, Instituto Universitario de Bio-Organica "Antonio González", Universidad de la Laguna, C/ Astrofísico Francisco Sánchez 2, 38206 La Laguna, Spain

^d Institute for Biological Research "Siniša Stanković", National Institute of the Republic of Serbia, University of Belgrade, Despota Stefana 142, 11108 Belgrade, Serbia

^e Dipartimento di Scienze della Salute, Università "Magna Græcia" di Catanzaro, Campus Universitario "S. Venuta", Viale Europa, 88100 Catanzaro, Italy

^f Net4Science Academic Spinoff, Università "Magna Græcia" di Catanzaro, Campus Universitario "S. Venuta", Viale Europa, 88100 Catanzaro, Italy

^g Associazione CRISEA – Centro di Ricerca e Servizi Avanzati per l'Innovazione Rurale, Località Condoleo, 88055 Belcastro (CZ), Italy

^h NEUROFARBA Department, Sezione di Scienze Farmaceutiche e Nutraceutiche, University of Florence, 50019 Florence, Italy

ARTICLE INFO

Keywords:

Coumarin
Mitochondriotropic agent
Carbonic anhydrase inhibitor
Cytostatic agent
Apoptosis

ABSTRACT

Being aware of the need to develop more efficient therapies against cancer, herein we disclose an innovative approach for the design of selective antiproliferative agents. We have accomplished the conjugation of a coumarin fragment with lipophilic cations (triphenylphosphonium salts, guanidinium) for providing mitochondriotropic agents that simultaneously target also carbonic anhydrases IX and XII, involved in the development and progression of cancer. The new compounds prepared herein turned out to be strong inhibitors of carbonic anhydrases IX and XII of human origin (low-to-mid nM range), also endowed with high selectivity, exhibiting negligible activity towards cytosolic CA isoforms. Key interactions with the enzyme were analysed using docking and molecular dynamics simulations.

Regarding their *in vitro* antiproliferative activities, an increase of the tether length connecting both pharmacophores led to a clear improvement in potency, reaching the submicromolar range for the lead compounds, and an outstanding selectivity towards tumour cell lines (S.I. up to >357). Cytotoxic effects were also analysed on MDR cell lines under hypoxic and normoxic conditions. Chemoresistance exhibited by phosphonium salts, and not by guanidines, against MDR cells was based on the fact that the former were found to be substrates of P-glycoprotein (P-gp), the pump responsible for extruding foreign chemicals; this situation was reversed by administrating tariquidar, a third generation P-gp inhibitor. Moreover, phosphonium salts provoked a profound depolarization of mitochondria membranes from tumour cells, thus probably compromising their oxidative metabolism.

To gain insight into the mode of action of title compounds, continuous live cell microscopy was employed; interestingly, this technique revealed two different antiproliferative mechanisms for both families of mitocans. Whereas phosphonium salts had a cytostatic effect, blocking cell division, guanidines led to cell death via apoptosis.

* Corresponding authors.

E-mail addresses: camala@ibiss.bg.ac.rs (M. Pešić), claudiu.supuran@unifi.it (C.T. Supuran), jmpadron@ull.es (J.M. Padrón), osc-lopez@us.es (Ó. López).

<https://doi.org/10.1016/j.bioorg.2024.107168>

Received 21 November 2023; Received in revised form 22 January 2024; Accepted 30 January 2024

Available online 6 February 2024

0045-2068/© 2024 The Author(s). Published by Elsevier Inc. This is an open access article under the CC BY-NC-ND license (<http://creativecommons.org/licenses/by-nc-nd/4.0/>).

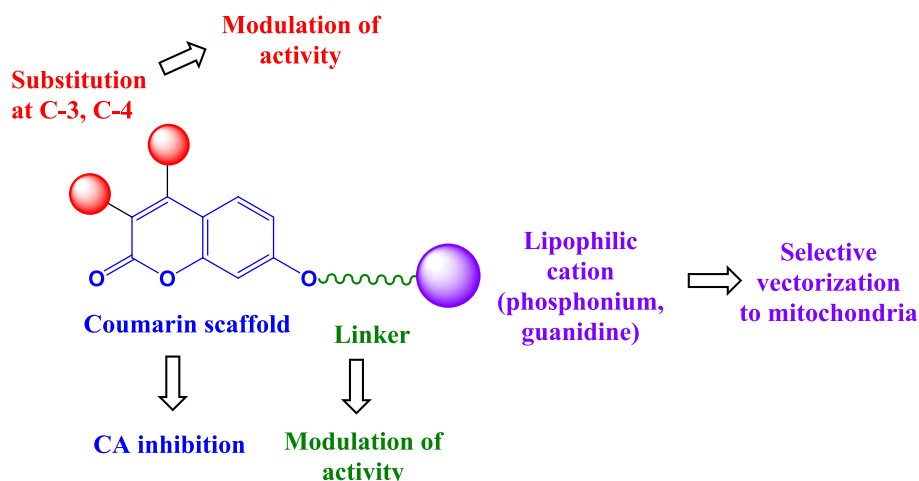
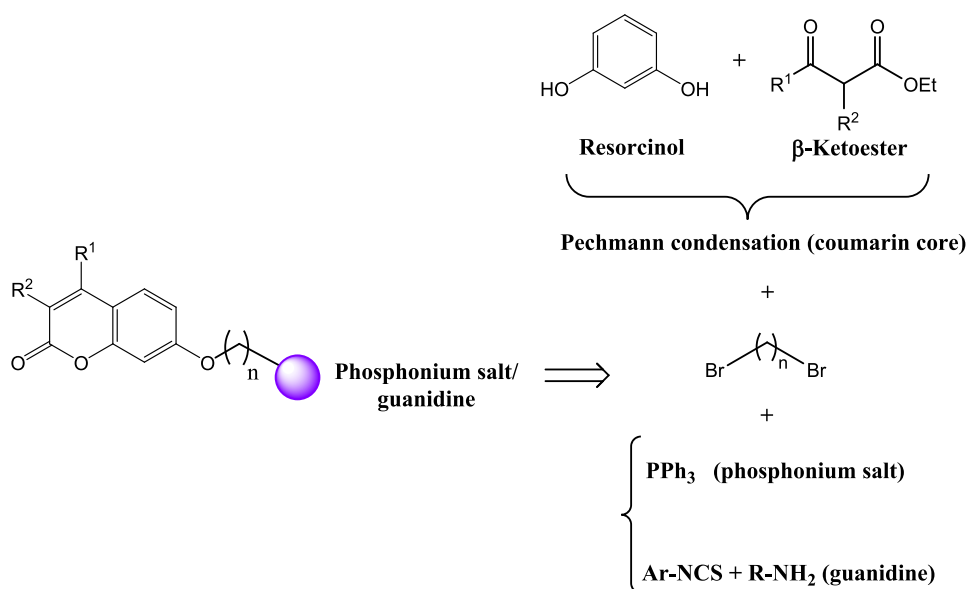


Fig. 1. Coumarin-lipophilic cations hybrids accessed herein.



Scheme 1. Retrosynthetic analysis for accessing targeted coumarin-appended phosphonium salts and guanidines.

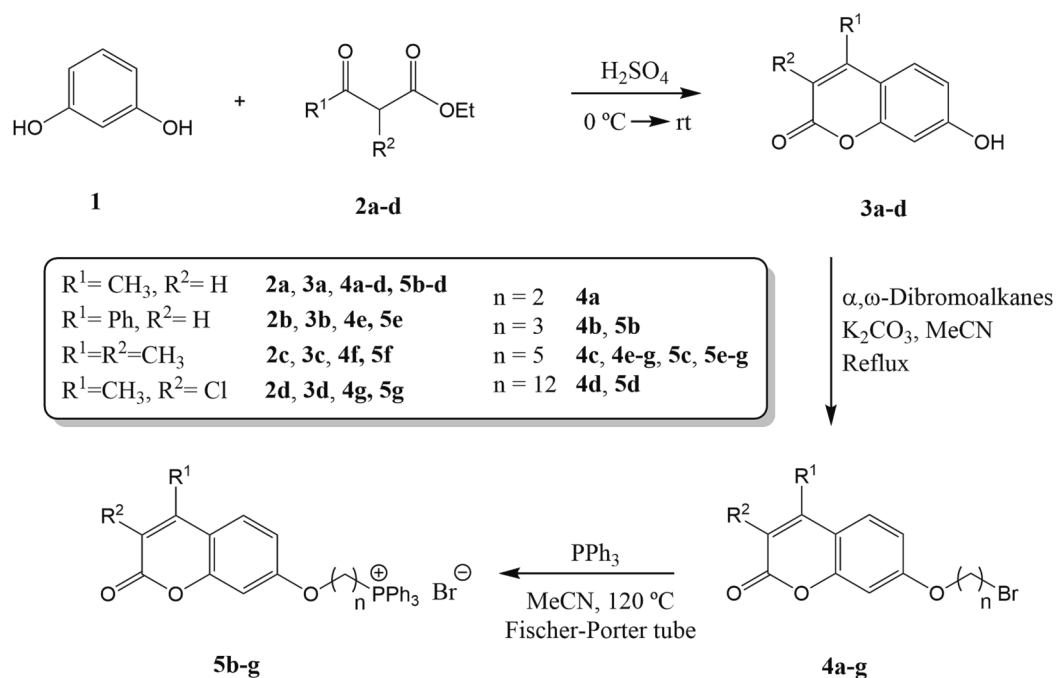
1. Introduction

Cancer is currently considered to be one most complex diseases [1], with an etiology not completely elucidated [2]. Undoubtedly, there have been outstanding advances in cancer treatment in the last few decades [3], both for therapeutic and diagnosis purposes. Thus, alone themselves, or combined with classical treatments (chemotherapy, radiotherapy, surgery), nanodelivery carriers (e.g. nanoparticles [4], extracellular vesicles [5]), adjuvants/neoadjuvants [6], targeted [7] and gene [8] therapies, magnetic hyperthermia [9], or immunotherapy [10], including cancer vaccines [11] and monoclonal antibodies [12] have increased life expectancy of patients. Despite that, most of the current treatments are still based on the use of chemotherapeutic agents, which in many occasions are devoid of selectivity, leading to severe side-effects [13], and also frequently undergo chemoresistance [14].

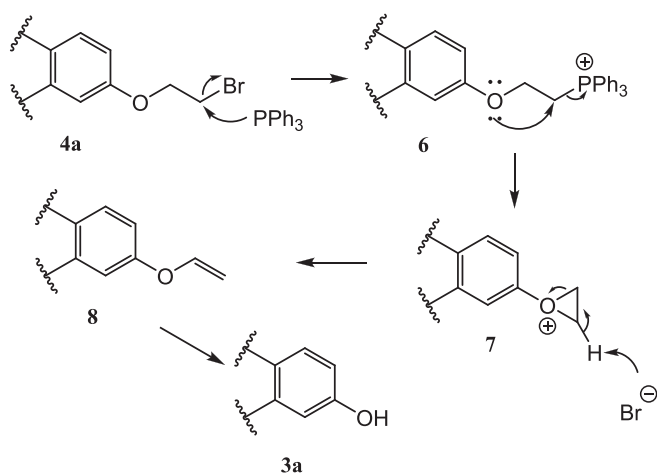
Among the numerous potential targets against cancer, mitochondria have become an attractive one in Medicinal Chemistry. Mitochondria are subcellular organelles that play key biological functions: they do not only produce ATP through the oxidative phosphorylation pathway, what constitutes 95 % of cell energy supply, but they also keep ion homeostasis, mediate in the biosynthesis of macromolecule

intermediates, regulate apoptosis, and scavenge Reactive Oxygen Species (ROS) [15]; moreover, there is a close relationship between dysfunctional mitochondria and tumorigenesis, through a complex crosstalk with other organelles [16].

This has triggered the development of drugs targeting mitochondria [17] which have been proved to be useful for diminishing the injuries caused by ischaemia, or for the treatment of inflammation, neurodegenerative and lung diseases, or cancer, among others. Compounds showing high affinity towards mitochondria, because of their particular physicochemical properties, are called mitochondriotropic agents [18]; when such compounds exhibit anticancer properties, they are called mitocans (*mitochondria + cancer*) [18,19]. Although there are a series of scaffolds acting as selective vehicles to mitochondria, like dequalinium vesicles, or mitochondria-penetrating peptides (e.g. Szeto-Schiller peptides), the most common ones are delocalized lipophilic cations (triphenylphosphonium (TPP⁺), guanidinium, rhodamine, heterocyclic aromatic cations) [18,20]; the latter ones, due to the large and negative mitochondrial membrane potential ($\Delta\Psi_{mit} = 150\text{--}180\text{ mV}$) compared to plasma ($\Delta\Psi_{plasma} = 30\text{--}60\text{ mV}$), largely accumulate within mitochondria matrix (up to 500-fold), according to the Nernst equation [20]. This effect is magnified in cancer cells, due to hyperpolarization of their



Scheme 2. Preparation of phosphonium salts 5b-g.



Scheme 3. Plausible mechanism for the spontaneous degradation of phosphonium derivative 6.

membranes [21].

Another target we have exploited herein are carbonic anhydrases (CAs); they comprise a series of metalloenzymes that usually bear Zn(II) as the prosthetic group. CAs catalyse CO_2 hydration to furnish $\text{HCO}_3^- + \text{H}^+$ [22], a crucial reaction within living beings. Within the phylogenetic tree, only a limited number of Gram-negative bacteria and one Archaeon lack CAs [22]. CAs are distributed along eight gene families [23], α -CA being the only one encoded in mammals along 15 different isoforms (12 of them catalytically active) [24], and take part in a plethora of biological pathways, like ureagenesis, gluconeogenesis, lipogenesis, pathogen virulence, and pH regulation [25]. The three remaining mammal isoforms (hCA VIII, X and XI) have no known biological role, and are known as CA-related proteins [26]. Currently, inhibition of CAs constitute a validated target for treating glaucoma [27], bacterial infections [28], obesity [29], or cancer [30]. Even, an involvement of CAs in Alzheimer's disease has been postulated [31]. In connection with cancer, SLC-0111, a ureido-containing sulfonamide was found to strongly

inhibit CA IX and XII isoforms; recently, it entered clinical trials (phase II) against pancreatic ductal adenocarcinoma with overexpression of CA IX, in a combination therapy [30]. α -CAs IX and XII are up-regulated in hypoxic metastatic tumours, promoting metastasis and tumour growth [30].

Herein, we envisioned the possibility of preparing new chemotherapeutic agents endowed with enhanced selectivity, and therefore, with potential reduced side-effects. For that purpose, an innovative dual-targeting approach has been followed, by combination of a mitochondria-targeted scaffold, which acts as a selective vehicle towards cancer cells mitochondria, and a pharmacophore acting on carbonic anhydrases (CAs).

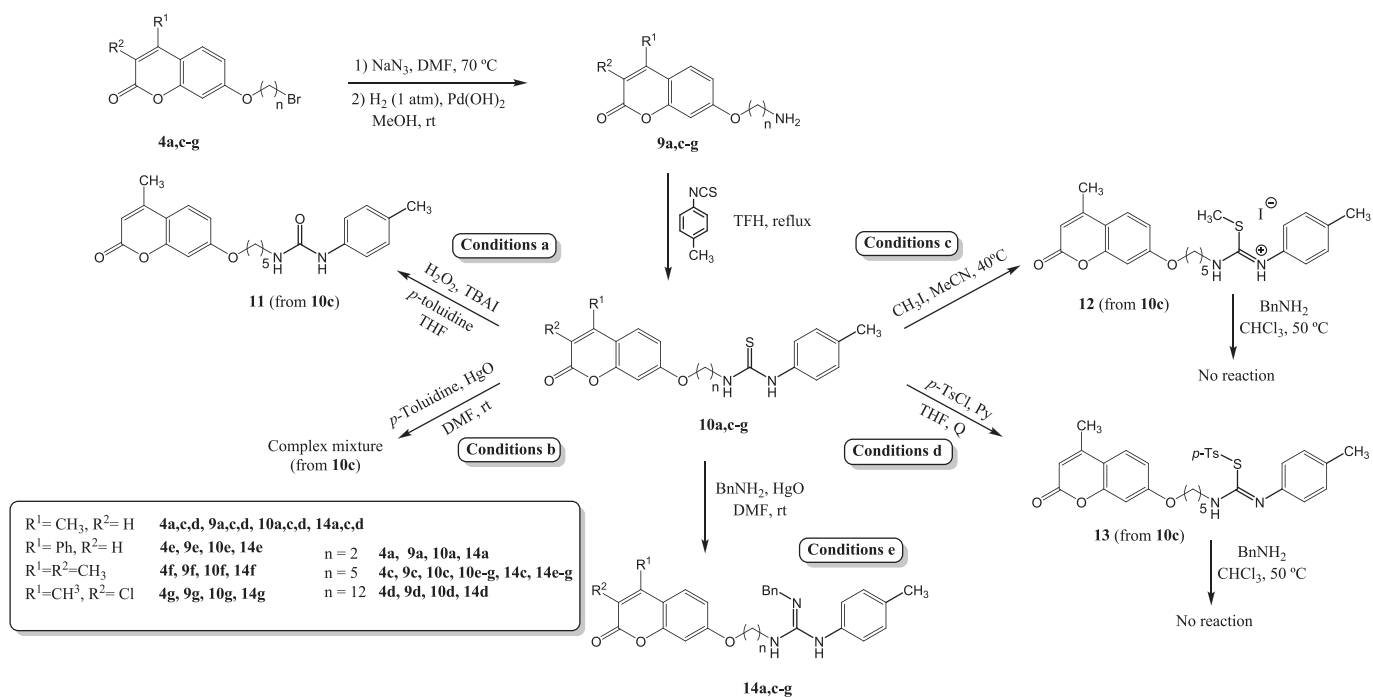
2. Results and discussion

2.1. Chemistry

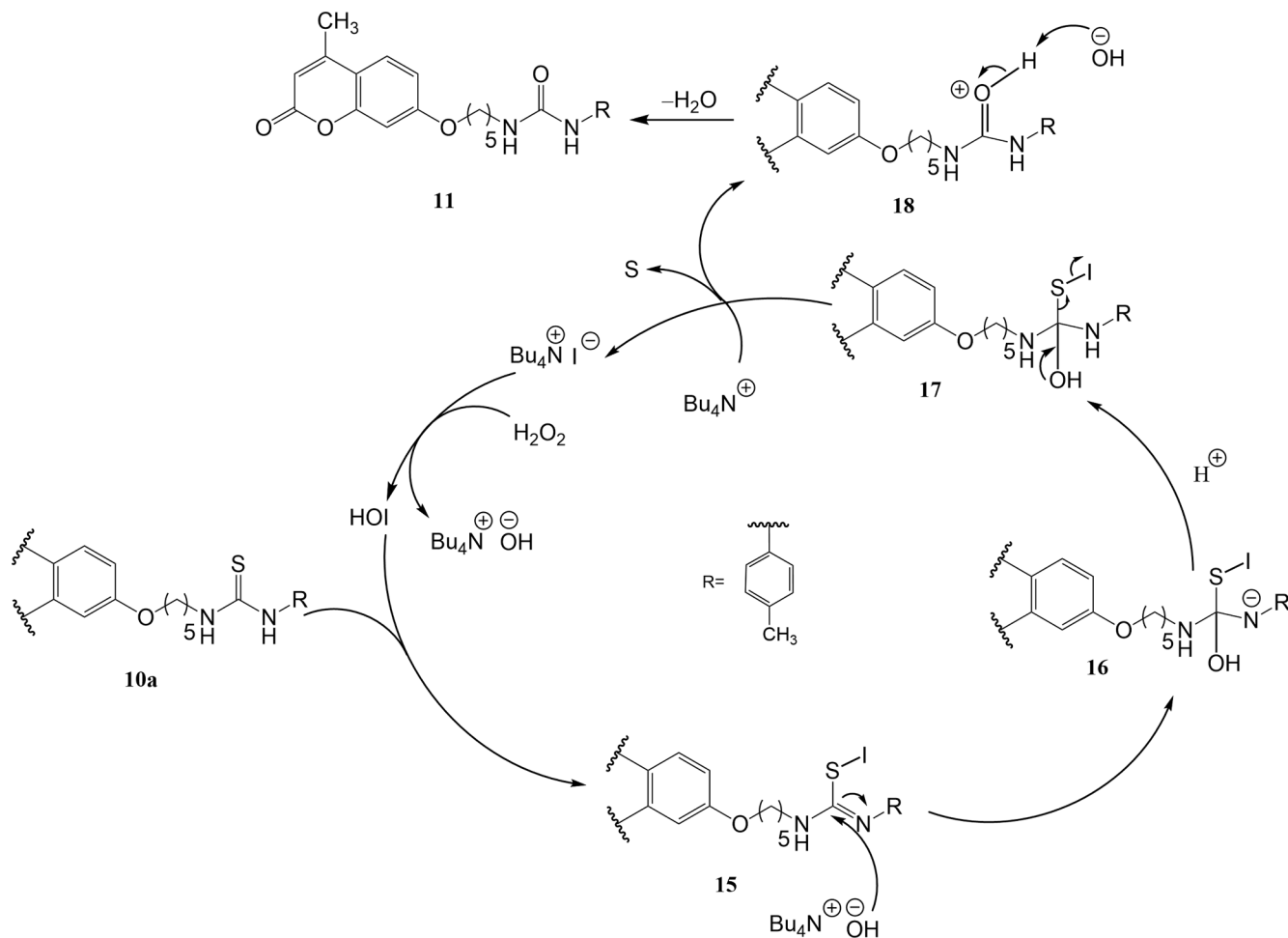
As aforementioned, in this manuscript we have appended a phosphonium salt or a guanidine scaffold (delocalized lipophilic cations) to a coumarin core for achieving a novel family of tumour-targeting compounds. With this kind of structure, we pursued a dual effect on tumour cells; on the one hand, the coumarin scaffold could selectively inhibit CAs involved in tumour progression, namely CA IX and XII. Although the most typical chemotype used for inhibiting this metalloenzymes are sulfonamides and their isosters, we have selected coumarins instead, due to their frequent high selectivity towards the tumour-associated CA isoforms [32,33]. The lipophilic cation could act as a vehicle for the selective vectorization of the drug to the tumour cells, and also cause disruption of mitochondrial membranes of malignant cells (Fig. 1).

Access to such kind of derivatives involves (Scheme 1) a Pechmann condensation [34] between resorcinol and different β -ketoesters for accessing the coumarin core; modification of C-3 and C-4 substituents might modulate the potency and selectivity in both, CA inhibition and antiproliferative properties. Moreover, it has also been reported that incorporation of alkyl residues on C-3 and C-4 can reduce the hepatotoxicity of this kind of compounds by hindering the P-450-mediated formation of transient coumarin 3,4-epoxides in their metabolic routes [35].

Subsequent O-alkylation with different α,ω -dibromoalkanes can

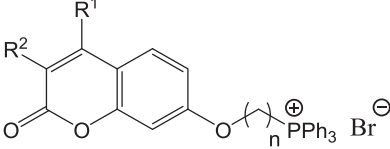
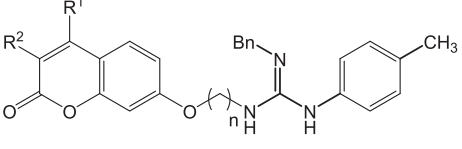


Scheme 4. Preparation of coumarin-derived guanidines 14a,c,g.



Scheme 5. Plausible mechanism for the formation of urea 11 via iodine-mediated desulfurization of thiourea 10c.

Table 1Inhibition constants (K_i , nM) of compounds **5**, **14** against hCAs I, II, IV, VII, IX, XII.

Compound	hCA I	hCA II	hCA IV	hCA VII	hCA IX	hCA XII
						
5b R ¹ = CH ₃ , R ² = H n = 3	>10000	>10000	794	>10000	82.5	80.6
5c R ¹ = CH ₃ , R ² = H n = 5	>10000	>10000	nt	nt	54.1	9.2
5d R ¹ = CH ₃ , R ² = H n = 12	>10000	>10000	689	>10000	460	88.3
5e R ¹ = Ph, R ² = H n = 5	>10000	>10000	796	>10000	408	89.3
5f R ¹ = R ² = CH ₃ n = 5	>10000	>10000	nt	nt	7.8	8.1
5g R ¹ = CH ₃ , R ² = Cl n = 5	>10000	>10000	nt	nt	7.9	58.2
						
14a R ¹ = CH ₃ , R ² = H n = 2	>10000	>10000	891	>10000	143	93.6
14c R ¹ = CH ₃ , R ² = H n = 5	>10000	>10000	nt	nt	8.1	619.1
14d R ¹ = CH ₃ , R ² = H n = 12	>10000	>10000	852	>10000	415	95.5
14e R ¹ = Ph, R ² = H n = 5	>10000	>10000	834	>10000	57.8	319
14f R ¹ = R ² = CH ₃ n = 5	>10000	>10000	958	>10000	685	54.5
14g R ¹ = CH ₃ , R ² = Cl n = 5	>10000	>10000	792	>10000	313	74.4
AAZ	250.0	12.0	74.0	2.5	25.0	5.7

nt: Not tested.

provide a flexible tether that might improve the fitting of the pharmacophore within hCA active site and improve the non-covalent interactions. This intermediate was used for the derivatization into phosphonium salts and guanidines, as depicted in Schemes 2 and 4.

Thus, the preparation of phosphonium salts **5b-g** is depicted in Scheme 2; reaction of resorcinol with β -ketoesters **2** catalysed by H₂SO₄ afforded coumarins **3**, either mono-substituted on C-4 position (**3a,b**), or disubstituted on C-3 and C-4 positions (**3c,d**). Subsequent Williamson etherification reaction under basic conditions (K₂CO₃) involving the free

OH on C-7 with an excess (10 equiv.) of a series of linear α,ω -dibromoalkanes (n = 2, 3, 5, 12) furnished bromo-derivatives **4a-g**. Biological properties might depend on the distance between the coumarin and the phosphonium moieties; moreover, increase of conformational flexibility might also favour the appropriate fitting within the CA active site.

Final nucleophilic displacement with PPh₃ on **4a-g** (Scheme 2) in acetonitrile using a Fischer-Porter tube (T = 120 °C) afforded phosphonium salts **5b-g** (59 %–quantitative yields).

Attempts to prepare the phosphonium salt with a 2-carbon tether (starting from bromo-coumarin **4a**) failed; unexpectedly, reaction of PPh₃ with **4a** using the reaction conditions depicted in Scheme 2 furnished coumarin **3a**, with loss of the bromoalkyl chain. Scheme 3 depicts the tentative mechanism for explaining such observation. Therefore, the anchimeric assistance of the oxygen atom on C-7 was considered, whose intramolecular nucleophilic attack on position C-2 of the ethyl chain would afford a transient charged-epoxide. Opening of such epoxide mediated by the bromide anion would lead to the formation of a vinyl ether that could be hydrolysed in the presence of the *in situ* generated HBr to give coumarin **3a**, with a free OH on C-7 position.

The presence of the triphenyl phosphonium moiety in **5b-g** was easily evidenced by NMR spectroscopy; thus, besides the incorporation of 15 aromatic protons in ¹H NMR spectra, phosphorous provoked the splitting of vicinal aromatic and aliphatic carbon signals.

For the preparation of coumarin-derived guanidines **14a,c-g**, we envisioned the use of thioureas **10a,c-g** as the key intermediates (Scheme 4). Such derivatives can be easily accessed starting from bromo-coumarins **4a,c-g** by first, NaN₃-promoted nucleophilic substitution, followed by heterogeneous hydrogenolysis and reaction of the transient terminal amine with commercially-available *p*-tolyl isothiocyanate (Scheme 4). Attempts to carry out the coupling with refluxing EtOH afforded **10c** in a 63 % yield with long reaction times (18 h) and partial degradation of the isothiocyanate. Changing the solvent to MeCN and rt provoked extensive degradation of the isothiocyanate and large amounts of remaining **9c** were observed. Shift to refluxing THF afforded **10c** in an excellent yield (82 %) and short reaction times (3 h); such optimized conditions were extended to the preparation of the remaining thioureas **10**. The formation of **10a,c-g** was evidenced by resonance at roughly 180 ppm in ¹³C NMR, attributed to the thioxo (C=S) group.

Once the thioureas were prepared, several conditions were attempted to optimize their transformation into targeted guanidines **14** upon a desulfurization step.

Firstly, thiourea **10a** was treated with H₂O₂ (Scheme 4, conditions a), in the presence of *p*-toluidine and tetrabutylammonium iodide (TBAI), under similar conditions reported [36] by Yadav and co-workers for the transformation of *o*-phenolic thioureas into 2-aminobenzoxazoles. Isosteric urea **11** was obtained in an acceptable yield (56 %) instead the expected guanidine. Scheme 5 depicts a plausible for the formation of such compound; reaction of H₂O₂ and TBAI furnishes hypiodous acid (HIO) which oxidizes the thioureido moiety to give iodinated derivative **15**. We postulate that instead of taking place the nucleophilic attack of *p*-toluidine, it was the more nucleophilic hydroxide anion from tetrabutylammonium hydroxide the one that reacted with **15** to yield intermediate **16**, which in turn after protonation, and loss of sulfur and iodide anion, evolved to urea **11**. NMR spectra clearly did not show incorporation of the *p*-toluidine fragment, and resonance of the quaternary carbon shifted from roughly 180 ppm (thiourea) to 156.7 ppm, typical for an ureido motif [37].

In order to avoid the generation of strongly basic conditions obtained by the above methodology, yellow HgO was used for the desulfurization reaction; in our research group, such reagent has been previously used for the preparation of 2-amino-1,3-oxazolines from carbohydrates [38,39] and steroids [40], and also ureas and guanidines derived from the natural sulfoaminoacid taurine [41]. In all cases, and starting from thioureas, reaction was proposed to proceed through a carbodiimide as the key intermediate. Treatment of thiourea **10c** with HgO and *p*-

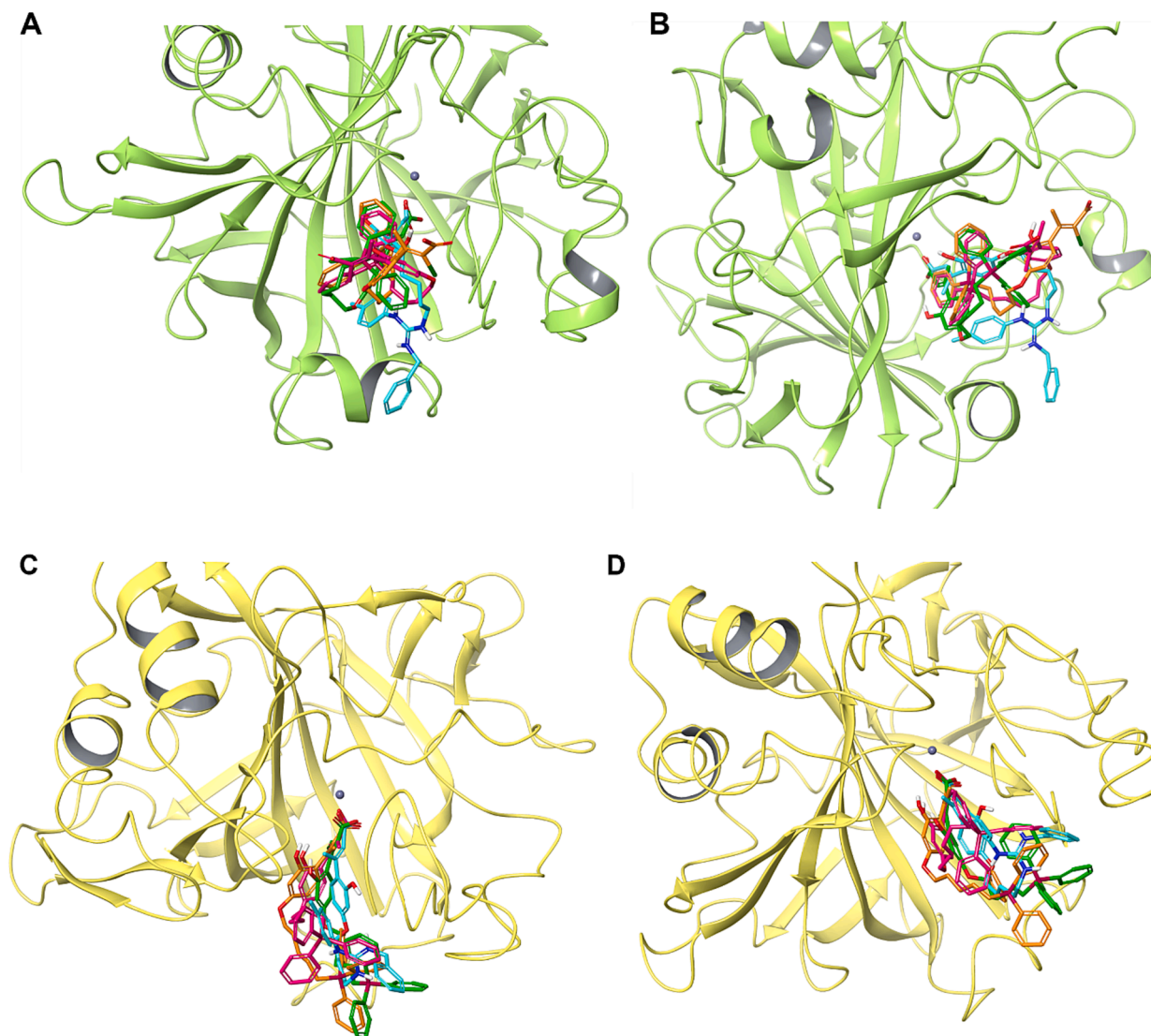


Fig. 2. Three-dimensional representation of hCA XII (faded green) and hCA IX (faded yellow) in complex with the model compounds **5c**, **f**, **g**, **14c**. In particular, (A, C) constitute the top views and (B, D), the side views of the ligands within the binding site. (For interpretation of the references to colour in this figure legend, the reader is referred to the web version of this article.)

Table 2

G-scores (kcal/mol) of the best dual hits related to both hCA isoforms for coumarins **5c**, **f**, **g**, **14c**.

Compound	hCA XII	hCA IX
5c	-6.658	-6.852
14c	-6.732	-5.952
5f	-4.410	-7.001
5g	-4.807	-6.581

toluidine afforded a more polar compound as evidenced by TLC, which was obtained in low yield and as a non-resolved mixture of compounds (Scheme 4, conditions b).

Considering that *p*-toluidine exhibits a moderate nucleophilicity to react with the intermediates generated upon the desulfurization reaction, it was replaced with benzylamine. To our delight, under these conditions (yellow HgO + BnNH₂), thiourea **10c** was successfully transformed into guanidine **14c** in an 84 % yield (Scheme 4, conditions e) after 66 h. Attempts to reduce the reaction time by the use of more reactive intermediates (*S*-methyl thiouronium salt [42] **12**, conditions c; tosylated thiourea [43] **13**, conditions d) failed, as no reaction was

observed (Scheme 4). Accordingly, conditions e from Scheme 4 were applied to the complete series of compounds, furnishing the corresponding guanidines **14a**, **c–g** in excellent yields (81 %–quantitative) after chromatographic purification. Resonance at roughly 151 ppm, and disappearance of the signal at 180 ppm (C=S) confirmed the proposed structures.

2.2. Biological assays

2.2.1. Carbonic anhydrase inhibition

The 12 mitochondria-directed derivatives prepared herein (phosphonium salts **5b–g**, and guanidines **14a**, **c–g**) were assayed as potential inhibitors of tumour-associated CAs, and their activities were compared with acetazolamide (AAZ, positive control). Cytosolic (I, II and VII), and membrane-bound (IV) enzymes were also tested to analyse the selectivity. Inhibition constants (*K_i*'s) were obtained (Table 1) from the stopped-flow CO₂ hydration protocol.

Data in Table 1 allowed the establishment of relevant structure–activity relationships:

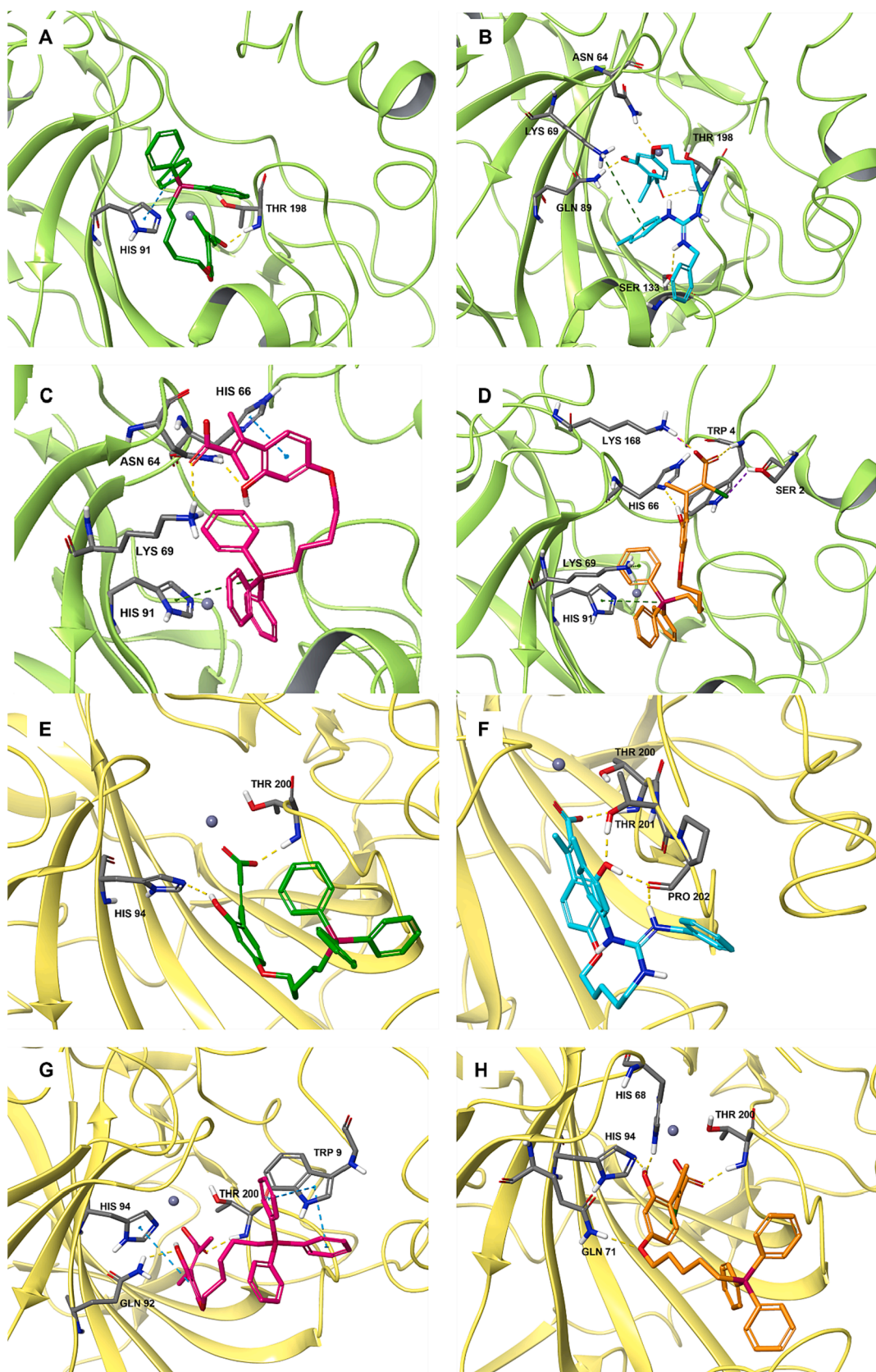


Fig. 3. 3D plots of the best poses of **5c** (A, E; green sticks), **14c** (B, F; cyan sticks), **5f** (C, G; magenta sticks), and **5g** (D, H; orange sticks) into the binding pockets of hCAs XII and IX. The ligands are shown in sticks, hCA IX and hCA XII are shown as a faded yellow-green and faded green ribbon respectively; the key enzyme residues interacting with title compounds are represented as grey carbon sticks. π -Cation, π - π stacking, halogen bond and hydrogen bonding interactions are indicated with dashed lines (green, cyan, violet, and yellow, respectively). (For interpretation of the references to colour in this figure legend, the reader is referred to the web version of this article.)

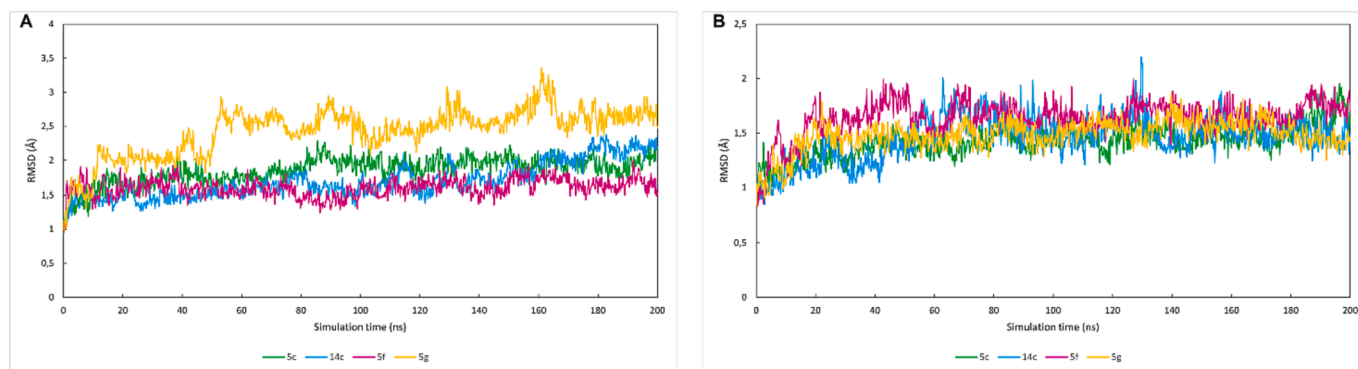


Fig. 4. RMSD (Å) trend obtained on the C α of hCA XII (A) and hCA IX (B), in complex with **5c** (green line), **14c** (cyan line), **5f** (magenta line), **5g** (orange line). (For interpretation of the references to colour in this figure legend, the reader is referred to the web version of this article.)

- i. Phosphonium salts **5** and guanidines **14** exhibited negligible activity towards cytosolic hCAs (I, II, VII; $K_i > 10,000$ nM for all cases). Submicromolar activities were found against CA IV.
- ii. Low-to-mid nM activities were found for the lead compounds against tumour-related CA IX and XII. Therefore, remarkable selectivities were found for such cases.
- iii. Regarding the influence of the tether length (compounds **5b-d** and **14a,c,d**), a five-carbon spacer was found to be optimal for inhibiting CA IX in both series of derivatives, and for inhibiting CA XII in the case of the phosphonium salts.
- iv. Concerning the influence of C-3 and C-4 substitution pattern, disubstitution on these positions with short alkyl fragments (Me) furnished the lead compound (**5f**), with $K_i = 7.8$ and 8.1 nM against CAs IX and XII, respectively. The use of a Ph residue on C-4 as a bulky substituent (**5e**) was detrimental for the inhibition of CA IX.
- v. In general, phosphonium bromides **5** were stronger CA inhibitors than guanidines **14**.
- vi. A considerable improvement in selectivity was achieved compared to AAZ, an arylsulfonamide in clinical use.

2.2.2. Docking simulations

In order to clarify the trends observed for the inhibitory potency of the designed derivatives against the CAs tested, molecular modelling studies were performed; for this purpose, compounds **5c,f,g**, **14c** were selected. Coumarins have been reported to act as suicide inhibitors of hCAs; they are hydrolysed within the enzyme cavity [44] to give 2-hydroxycinnamic acid derivatives which are the actual derivatives occluding the CA cavity entrance [32]. Initially, docking poses and docking scores were evaluated (Fig. 2, Table 2); all compounds showed binding energy values comparable to the ones obtained for known inhibitors (Table S1). Strong interactions with hCA IX and XII binding pocket residues were found, what was evidenced by the high number of contacts detected using the Maestro interface [45] (Tables S2, S3).

In connection with hCA XII, the open form of compound **5c** established a H-bonding interaction between the COOH moiety and Thr198, a π - π stacking interaction involving the aryl residue of the triphenylphosphonium group, and two different electrostatic interactions between the oxygen atoms of the COOH group and the metal cation (Fig. 3A). In a very similar manner, regarding hCA IX, the open form of compound **5c** formed a H-bonding interaction between COOH and Thr200, and a further H-bond between the phenolic hydroxyl group and His94; additionally, two electrostatic interactions between COOH and the Zn²⁺ ion were also found (Fig. 3E). The same interactions were also found for compound **14c** in both isoforms, but due to the structural diversity of the two molecules, **14c** is further stabilised by several additional interactions, specifically a H-bonding interaction between the phenolic hydroxyl group and Gln89, a H-bond interaction between the ether group oxygen and Asn64, a H-bond between the NH⁺ residue and

Ser133, a π -cation interaction involving the methyl group of the tolyl moiety and Lys69 in hCA XII (Fig. 3B). In hCA IX, the additional interactions involve the phenolic hydroxyl group, which establishes a two different H-bond with Thr201 and Pro202; moreover, Pro202 also establishes another H-bond with NH⁺ (Fig. 3F).

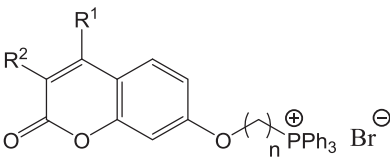
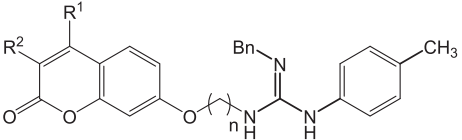
With regard to the open forms of compounds **5f** and **5g**, there are substantial differences between the two isoforms; in hCA XII they arrange the triphenylphosphonium cation within the binding site and the coumarin moiety outside the site, whereas in hCA IX they continue to arrange themselves with the same binding mode observed for **5c**. Specifically, in hCA XII, **5f** forms a π -cation interaction between P⁺ and His91, a π - π stacking interaction involving the coumarin scaffold and His66, a H-bond between the free OH on the coumarin residue and Asn64, a H-bond between the carbonyl group of the carboxylic acid moiety and Lys69 (Fig. 3C). In contrast, in hCA IX, **5f** forms three different π - π stacking interactions, including one between the coumarin phenyl residue and His94 and two between the central and one lateral aromatic ring of the triphenylphosphonium salt and Trp9. It also establishes a H-bond between the phenolic hydroxyl group and Gln92 and a H-bond involving the carbonyl group of the carboxylic acid moiety and Thr200; in addition, two electrostatic interactions are also formed between the carboxylic group and the Zn²⁺ ion (Fig. 3G).

Finally, considering hCA XII, **5g** establishes two π -cation interactions, one between P⁺ and His91 and one between the central ring of the triphenylphosphonium salt and Lys69, several H-bonds, specifically, one between the phenolic hydroxyl group and His66 and one between the carbonyl group from the COOH moiety and Trp4, a halogen interaction between the chlorine atom and Ser2, and a salt bridge between the hydroxyl of the carboxylic acid moiety and Lys168 (Fig. 3D). In contrast, in hCA IX, **5g** forms 4 different H-bonds, including one between the carbonyl of the COOH moiety and Thr200, one between the ether group oxygen and Gln71, and two different ones between the phenolic hydroxyl group, His68 and His94; again, two electrostatic interactions between the carboxylic acid and the Zn²⁺ ion were also found (Fig. 3H).

Subsequently, the different binding modes and interactions were further investigated through molecular dynamics studies. As far as **5c** is concerned, after an initial settling period, it forms a sufficiently stable complex in both isoforms with fluctuations expressed in terms of RMSD that are maintained in the range of 2 Å (Fig. 4). In hCA XII, **5c** is stabilised by interactions formed during the course of the dynamics with residues His93, Glu104, Thr198 and that are maintained throughout the simulation time. In hCA IX, the complex is strongly stabilised by a large number of interactions that are maintained almost throughout the course of the dynamics, again establishing more than one contact with the same residue, and in particular with Tyr11, Asn66, His96, Glu106, Thr200, Thr201.

A similar situation is evidenced by the interaction of **14c** with both isoforms, which in both cases forms two stable complexes, characterised

Table 3
Antiproliferative activity of compounds **5**, **14**.

Compound	GI ₅₀ (μM)						LC ₅₀ (μM)
	A549 (non-small cell lung) Sensitive lines	HBL-100 (breast)	HeLa (cervix)	SW1573 (non-small cell lung)	T-47D (breast) Multidrug resistant lines	WiDr (colon) Multidrug resistant lines	BJ-hTERT (human fibroblasts) Non-tumour
							
5b R ¹ =CH ₃ , R ² =H n = 3	5.5±0.9	20±3	11±1	16±1	24±1	25±3	n.t.
5c R ¹ =CH ₃ , R ² =H n = 5	2.1±0.9	3.9±0.3	3.8±1.1	2.7±0.6	3.6±0.4	3.4±0.4	>100
5d R ¹ =CH ₃ , R ² =H n = 12	0.36±0.08	0.44±0.09	0.32±0.10	0.28±0.06	0.29±0.06	0.32±0.05	>100
5e R ¹ =Ph, R ² = H n = 5	1.6±0.4	1.1±0.3	0.60±0.14	0.95±0.14	0.72±0.32	0.58±0.19	>100
5f R ¹ =R ² = CH ₃ n = 5	2.8±0.8	3.0±1.0	2.1±0.1	2.2±0.7	2.4±0.1	2.6±0.7	>100
5g R ¹ = CH ₃ , R ² =Cl n = 5	2.5±0.4	1.5±0.4	1.6±0.5	1.5±0.4	2.5±1.1	2.6±0.7	>100
							
14a R ¹ =CH ₃ , R ² =H n = 2	13±3	15±1	13±1	8.8±1.6	5.2±0.6	4.5±0.1	n.t.
14c R ¹ =CH ₃ , R ² =H n = 5	6.4±3.1	9.0±2.3	3.8±1.3	6.1±2.0	3.4±0.3	2.8±0.4	>100
14d R ¹ =CH ₃ , R ² =H n = 12	1.2±0.1	1.3±0.2	0.85±0.21	0.81±0.09	0.87±0.22	0.41±0.06	>100
14e R ¹ =Ph, R ² = H n = 5	1.8±0.2	1.8±0.1	1.7±0.1	1.4±0.1	1.1±0.1	0.46±0.30	>100
14f R ¹ =R ² = CH ₃ n = 5	2.0±0.3	2.0±0.1	2.0±0.3	1.9±0.4	1.9±0.3	1.3±0.2	>100
14g R ¹ = CH ₃ , R ² =Cl n = 5	1.8±0.1	1.7±0.1	1.7±0.1	1.4±0.1	1.5±0.1	0.90±0.28	>100

n.t.: Not tested.

by not very pronounced fluctuations; in fact, a conspicuous number of stabilising interactions are formed and maintained throughout the 200 ns simulation, in particular with Tyr6, Gln89, His93, Glu104, Thr198 in hCA XII and with residues His94, His96, Glu106, His119, Thr200 and Thr201 in hCA IX.

As aforementioned, important differences in binding mode with the two isoforms can be seen for compound **5f**. In particular, in hCA XII, through the graphic visualisation of the trajectory, the movement of the ligand can be seen, which rotates until the coumarin portion is disposed in the binding site, leaving the triphenylphosphonium moiety on the outside. Although this does not affect the stability of the protein, which is maintained throughout, it justifies not only the fluctuations, but also the number of interactions with Thr199, one of the key residues in the binding pocket, which intensify after the first 100 ns of the dynamics. In contrast, in hCA IX, the ligand is stable within the binding site due to the

interactions that form several contacts with residues His96, Glu106, Thr200, Thr201 and are maintained for more than 98 % of the duration of the entire molecular dynamics. This same situation also occurs for compound **5g**; in this case, it can be seen that initially in hCA XII the ligand arranges the triphenylphosphonium group in the binding site and that subsequently there is a reversal of the binding mode which allows the coumarin portion to enter the pocket as demonstrated by visual inspection; after the first 150 ns of the simulation, the contacts with residues Thr199 intensify. As is the case for **5f**, also for **5g** in hCA IX the complex remains stable thanks to the various contacts established with His96, Glu106, Thr200 maintained for over 97 % of the entire simulation.

2.2.3. Antiproliferative activities

Potential antiproliferative activities of phosphonium bromides **5** and

Table 4Cytotoxicity of CA inhibitors in normoxic and hypoxic conditions (IC₅₀ ± SE, μM).

Conditions	Cell line	5c	5f	5g	14c
20 % O ₂	U87	5.574 ± 0.167	1.350 ± 0.323	1.843 ± 0.092	3.159 ± 0.192
		U87-TxR	30.551 ± 1.055	8.218 ± 1.372	11.410 ± 0.466
	<i>RRF^{a1}</i>	5.4	7.2	6.2	1.7
	1 % O ₂	U87	10.343 ± 1.683	9.586 ± 1.355	2.860 ± 1.707
U87-TxR			32.148 ± 1.240	13.616 ± 1.272	13.978 ± 1.636
<i>RRF^{a2}</i>		3.1	1.4	4.9	1.4
<i>RDH^b</i>		1.9	7.1	1.5	1.3
20 % O ₂	NCI-H460	3.129 ± 0.039	1.833 ± 0.521	2.618 ± 0.219	4.830 ± 0.501
		NCI-H460/R	27.588 ± 0.184	21.176 ± 0.070	33.973 ± 2.533
	<i>RRF^{d1}</i>	8.8	11.5	13.0	1.5
	1 % O ₂	NCI-H460	4.784 ± 1.185	2.548 ± 1.231	3.248 ± 1.258
NCI-H460/R			38.707 ± 1.286	24.615 ± 1.191	30.320 ± 1.241
<i>RRF^{d2}</i>		8.1	9.7	9.3	1.1
<i>RDH^e</i>		1.5	1.4	1.2	1.3
	<i>RDH^f</i>	1.4	1.2	0.9	0.9

^{a1,2}RRF = relative resistance factor, calculated as RRF = IC₅₀[U87-TxR]/IC₅₀[U87].^bRDH = resistance due to hypoxia, calculated as RDH = IC₅₀[U871%O₂]/IC₅₀[U8720%O₂].^cRDH = resistance due to hypoxia, calculated as RDH = IC₅₀[U87-TxR1%O₂]/IC₅₀[U87-TxR20%O₂].^{d1,2}RRF = relative resistance factor, calculated as RRF = IC₅₀[NCI-H460/R]/IC₅₀[NCI-H460].^eRDH = resistance due to hypoxia, calculated as RDH = IC₅₀[NCI-H4601%O₂]/IC₅₀[NCI-H46020%O₂].^fRDH = resistance due to hypoxia, calculated as RDH = IC₅₀[NCI-H460/R1%O₂]/IC₅₀[NCI-H460/R20%O₂].

guanidines **14** were evaluated against the tumour cell lines of human origin depicted in Table 3 (GI₅₀, μM). Furthermore, BJ-hTERT (non-tumour, human fibroblasts) was also included for analysing the cytotoxicity (expressed as LC₅₀) of the most potent compounds. Cisplatin (CDDP) and 5-fluorouracil (5-FU) were used as drug references.

Table 3 afforded the following structure–activity relationships:

- The use of longer tethers in both families of coumarin derivatives (phosphonium salts, guanidines), clearly improved the anti-proliferative activity, affording GI₅₀ values within the sub-micromolar range for n = 12 (0.28–0.44 μM for **5d**; 0.41–1.3 μM for **14d**).
- Disubstitution on positions C-3, C-4 (R¹ = R² = Me; R¹ = Me, R² = Cl) afforded virtually the same potency for phosphonium salts (**5c** vs. **5f**, **5g**) and an a moderate-to good improvement for guanidines (**14c** vs. **14f**, **14g**).
- When C-4 position of the coumarin core was substituted with a Ph residue, an improvement of potency in phosphonium salts (**5c** vs. **5e**) and guanidines (**14c** vs. **14e**) was obtained; up to a 6-fold improvement of GI₅₀ values was achieved.
- Remarkable selectivity was observed due to LC₅₀ > 100 μM for the BJ-hTERT cell line (non tumour, human fibroblasts), thus affording selectivity indexes of up to >357.

2.2.3.1. Cytotoxic effects of CA inhibitors on multidrug-resistant (MDR) cancer cells (hypoxic and normoxic conditions). The coumarin derivatives **5c,f,g** and **14c**, showing considerable inhibitory potential against CAIX and/or CAXII, were chosen for investigating the cytotoxic effect on

sensitive and MDR cells. For this purpose, two pairs of models of MDR cancer cells were used, the non-small cell lung carcinoma (NSCLC) sensitive NCI-H60 and resistant NCI-H460/R cells, and glioblastoma sensitive U87 and resistant U87-TxR cells. Importantly, MDR cells (NCI-H460/R and U87-TxR) possess overexpression of P-gp [46,47] whose functioning is tightly connected with CAIX and CAXII activity [48–51].

First, a SRB (sulforhodamine B) assay (48 h treatment) was used to assess the cell growth inhibition effects of **5c,f,g** and **14c** on the MDR cancer cell line models and their corresponding sensitive cancer cell lines. The assay was conducted under different O₂ growth conditions, simulating a normoxic and hypoxic environment (20 % and 1 % O₂, respectively, Table 4).

Under normoxic conditions (20 % O₂), all four compounds inhibited cell growth in resistant and sensitive cells, with IC₅₀ values up to 13 times higher in MDR cancer cells, compared to the sensitive cells (Table 4). The resilience to treatment indicates that the MDR phenotype is related to the CA inhibitor cytotoxic potency, similarly to previous research on coumarin derivatives in the same MDR models [50]. Although the resistance to treatment was obvious in the case of phosphonium salts (**5c,f,g**), the guanidine compound **14c** had a similar cytotoxic response in MDR and sensitive cancer cells. The most prominent growth inhibition effect was observed with **5f** –IC₅₀ values were found to be 1.35 μM for U87 and 1.83 μM for NCI-H460.

The cytotoxic response to CAIX and/or CAXII inhibitors was analysed under hypoxic conditions as well. Hypoxia is a common feature of solid cancers, given that uncontrolled tumour tissue growth is not perfectly harmonized to the tumour oxygen supply [52,53]. Consequently, oxygen and nutrient delivery to the tumour is inconsistent, causing major hypoxic and oxidative stress. The tumour cell adaptive response includes increased expression of pH-regulating and antioxidant enzymes induced by hypoxia-inducible factor 1α (HIF-1α) [54]. The major regulators of intracellular pH (pHi) are CAIX and CAXII, often upregulated in various tumour types [55,56]. In Table 4, it is notable how both lung cancer and glioblastoma cells under low oxygen conditions had increased IC₅₀ values for the tested compounds, compared to normoxia and the difference in IC₅₀ values was expressed as “resistance due to hypoxia” or RDH. The difference was most prominent in U87 when treated with **5f**, with RDH around 7 (Table 4). This higher resilience to the compounds was expected, as the activity of CAs is higher under hypoxic conditions [57,58]. Contrary, the response of the MDR cancer cells was similar under differing O₂ conditions – the greatest variance was for **5f** in U87-TxR growing at 1 % O₂, compared to 20 % O₂ (1.7 times higher IC₅₀ value, Table 4). Activity of both CAIX and CAXII play a significant role in chemoresistance of MDR by enhancing P-gp efflux activity. Therefore, inhibiting CAs can help to reduce P-gp activity, which in turn can lead to a decrease in intracellular pH, ATP production and metabolic reprogramming of MDR cancer cells [48–51]. Particularly interesting result is that hypoxic condition did not affect the efficacy of **5c,f,g** and **14c** in the MDR cancer cells with P-gp overexpression. This implies that our CA inhibitors can be valuable in fight against cancer multidrug resistance. We cannot rule out the possibility that P-gp activity itself also stimulates CA activity in normoxic conditions. To assess whether the compounds are selective toward cancer cells, the growth inhibition effect of the four compounds (**5c,f,g** and **14c**) was also assayed in a normal lung cell line, MRC-5, as well. The inhibitory profiles and calculated Relative Selectivity Factor (RSF, Fig. 5a) clearly indicate compounds selectivity toward lung cancer cells, with NCI-H460 being up to around 10 times more sensitive to the compounds cytotoxic effect, compared to MRC-5.

Further on, cell death induction in NCI-H460 and MRC-5 was analysed by the Annexin V/Propidium Iodide staining (AV/PI, Fig. 5b,c). The cells were exposed to 10-μM phosphonium salts (**5c,f,g**) and 25-μM guanidine **14c** for 48 h. A significant increase in PI fluorescence in NCI-H460 indicates a dominantly necrotic cell death (Fig. 5b). Adversely, cell death was completely absent in MRC-5 cells (Fig. 5c). As Fig. 5 shows, the AV/PI assay confirmed the compounds were remarkably more toxic in malignant cells than in normal human cells – the above-

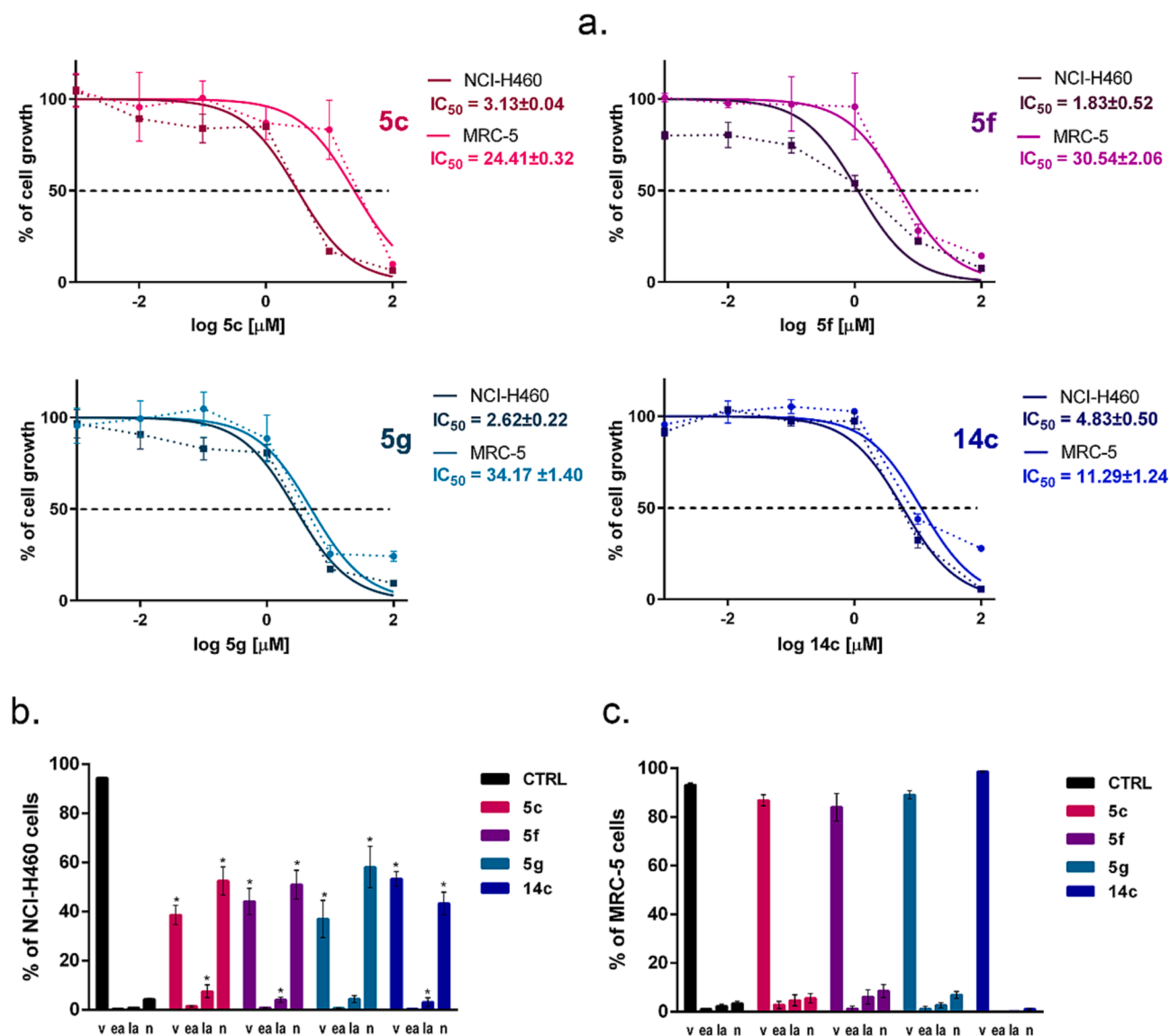


Fig. 5. Selectivity of coumarin derivatives toward cancer cells studied by SRB and cell death induction assays. (a) Growth inhibition of human NSCLC (NCI-H460) and lung fibroblasts (MRC-5) was assessed by sulforhodamin B assay (48 h); five different concentrations of the tested compounds were used: 10, 100 nM, 1, 10, and 100 μM. Data are presented as mean values ± SEM (n = 4). Nonlinear regression was obtained by GraphPad Prism 6. Relative selectivity factor (RSF) was calculated as $RSF = IC_{50}[NCI-H460]/IC_{50}[MRC-5]$. RSF for **5c** was 7.8, for **5f** is 16.7, for **5g** is 13.4, and for **14c** 2.3. (b) AV/PI staining was used for evaluating cell death (48 h treatment; 10 μM for compounds **5c,f,g**; 25 μM for **14c**), in NCI-H460 and MRC-5 cell lines. la: late apoptosis; ea: early apoptosis; n: necrosis; v: viable. Mann-Whitney test was employed for determining the statistical significance; * ($p < 0.05$) reveals a significant difference compared to control. Mean values ± SE (n = 3).

mentioned concentrations reduced cancer cell viability down to 40–50 %, while the application of the same concentrations resulted in 80 % viability of normal cells (Fig. 5b, c).

2.2.3.2. Chemosensitization of the MDR cancer cells to phosphonium salts. It seems that the P-glycoprotein activity contributes to the MDR cancer cell higher resilience to coumarin derivatives, compared with sensitive-pair cells. To provide an evidence, we applied an P-gp inhibitor simultaneously with coumarin derivatives in order to sensitize the MDR cancer cells. On that account, SRB assay was performed to analyse cell growth, following 48 h treatment with the CA inhibitors, along with the third generation P-gp inhibitor tariquidar (TQ) [59]. The results, presented in Fig. 6, confirmed that the phosphonium salts **5c,f,g** are substrates for the extruding pump since the simultaneous treatment with the tested compounds and TQ sensitized NCI-H460/R and U87-TxR cells (the MDR cancer cells) to the cytotoxic effect (Fig. 6a and b,

respectively).

On top of that, the simultaneous treatment of the guanidine compound **14c** with the P-gp inhibitor did not cause a remarkable change in cytotoxicity (Fig. 6a, b), which is in accordance with the insignificant difference between IC₅₀ values for **14c** in MDR and sensitive cancer cells obtained by SRB assay. This suggests that probably guanidine-containing coumarins are not substrates of the P-gp, thus not causing chemoresistance through extrusion of the drug mediated by this pump.

2.2.3.3. Coumarin derivatives depolarize mitochondria in NSCLC and glioblastoma cells. Intracellular acidification of cancer cells by CAs inhibitors could affect mitochondria activity. To that end, TMRE (tetramethylrhodamine ethyl ester perchlorate) was used as a fluorescent dye, in order to reveal changes in mitochondrial membrane potential. The tested compounds depolarized mitochondria, thus compromising the oxidative metabolism of cancer cells (Fig. 7). Maximal depolarization in

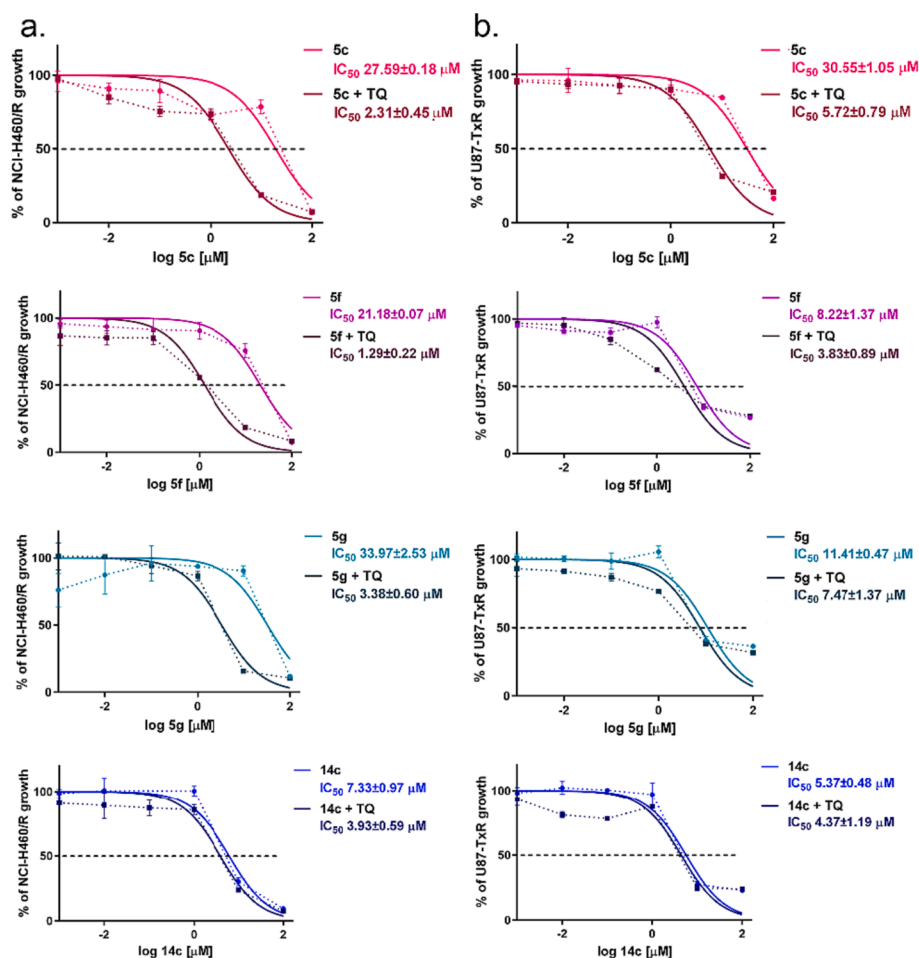


Fig. 6. TQ sensitizes the MDR cancer cells to CA inhibitors. Effects on NCI-H460/R (a) and U87-TxR cells provoked by **5c**, **f**, **g** and **14c** combined with TQ (50 nM) (b) cell growth (sulforhodamine B assay, 48 h). The effects were compared to single **5c**, **f**, **g** and **14c** treatments (U87-TxR and NCI-H460/R cells): 10, 100 nM, 1 10, and 100 μM concentrations. Data are presented as mean values ± SEM (n = 4). Nonlinear regression was obtained by GraphPad Prism 6.

lung cancer cells was caused by the phosphonium salt **5f** – around a 50 % decrease in TMRE fluorescence intensity was observed compared to the control experiment (Fig. 7a). The depolarizing effect was higher in glioblastoma cells (Fig. 7b), with the most prominent changes caused by **5f**, **g**, decreasing the mitochondrial activity by 75 % to 80 %, relative to the untreated control.

2.2.4. Continuous live cell imaging reveals a differential mode of action between phosphonium and guanidinium coumarins

To gain insight into the mechanism of the derivatives under study, SW1573 lung cancer cultures were followed by continuous live cell microscopy (Videos S1–S3). We selected for this test the phosphonium salt **5g** and the guanidinium derivative **14c**. SW1573 cells were exposed for 15 h at a dose corresponding to the total growth inhibition (TGI), i.e. 3 and 21 μM for **5g** and **14c**, respectively. Cell cultures were monitored every 3 min (label-free holotomographic 3D microscopy) [60]; such data can be found as Supplementary videos S1-S3. This technique allows to observe differences in the response of individual cells within a population. In SW1573 cells exposed to the phosphonium derivative **5g**, a cytostatic effect was observed. Cells showed a reduced motility and did not divide when compared to control cells (Fig. 8A). However, the exposure to guanidinium **14c** induced cell death, and several apoptotic markers could be observed. The phenotypic parameters total dry mass (Fig. 8B) and granularity (Fig. 8C) computed for each test showed a remarkable difference in the effects induced by the treatments. The kinetics of cell death allowed to differentiate the mode of action of both derivatives (Fig. 8D).

3. Conclusions

Two innovative families of mitocans with dual activities have been developed, by combination of a coumarin scaffold with different substitution pattern on C-3 and C-4 (for addressing cancer-related CAs IX and XII) and a positively-charged lipophilic moiety (phosphonium salt, guanidine), for the selective vectorization towards malignant cells. Derivatives with a methyl residue on C-4, or bearing two substituents on C-3 and C-4 (Me/Me, Cl/Me), and a pentyl-type linker turned out to be very strong CAs IX and XII inhibitors, low-to-mid nM range, and outstanding selectivities. Dimethylated coumarin **5f** was the lead inhibitor, with $K_i = 7.8$ and 8.1 nM against CA IX and XII, respectively.

Initial screening against six human tumour cell lines showed strong *in vitro* antiproliferative properties (submicromolar-low micromolar range), with improved potency upon increase distance between both pharmacophores, and excellent selectivity ($LC_{50} > 100$ μM against human fibroblasts).

The most relevant compounds (phosphonium salts **5c**, **f**, **g** and guanidine **14c**) were selected to get insight into their mode of action against malignant cells. Drug-sensitive and their multidrug resistant counterparts were used as MDR cell models; the antiproliferative assays were conducted under normoxic and hypoxic conditions. These assays revealed that phosphonium salt exhibited chemoresistance, acting as P-gp substrates, a situation that was reversed by co-administration with the third-generation inhibitor of P-gp tariquidar. Remarkably, related guanidines were devoid of such chemoresistance mechanism. Moreover, phosphonium salts provoked an extensive depolarization of

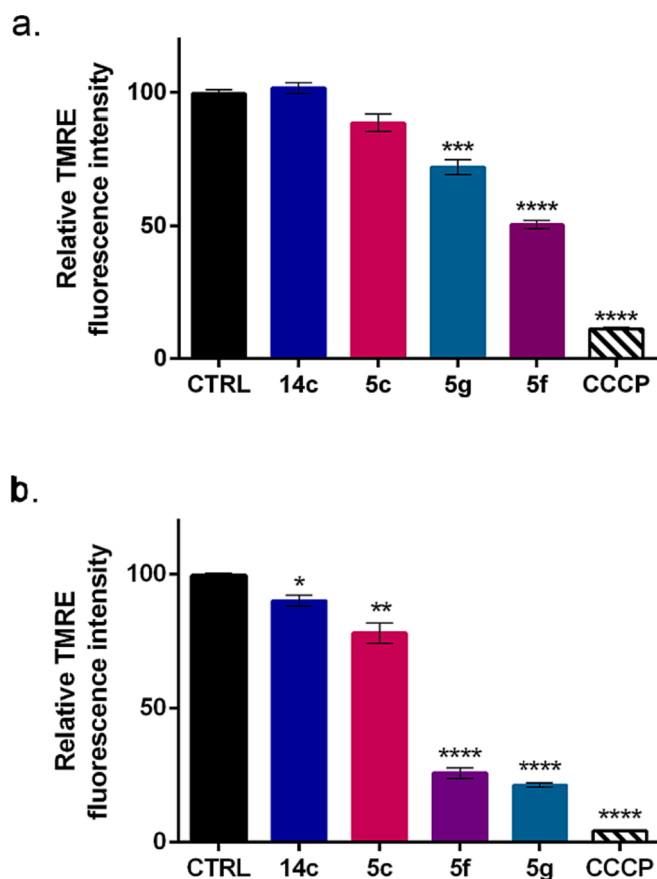


Fig. 7. CA inhibitors cause decreased mitochondrial activity. The mitochondrial activity in NCI-H460 (a) and U87 (b) cells was analysed with TMRE fluorescent dye, after 24 h treatment with 5c,f,g and 14c (concentrations \leq IC₅₀). CCCP was employed as control (10 μ M). An unpaired *t*-test using the Welch's correction was employed for obtaining the statistical significance: **** ($p < 0.0001$), *** ($p < 0.001$), ** ($p < 0.01$), * ($p < 0.05$). Mean values \pm SE ($n = 3$).

mitochondria membranes from cancer cells, and thus, probably compromising their oxidative metabolism.

Continuous live cell microscopy was employed to gain insight into the antiproliferative mode of action of title derivatives. Interestingly, two different mechanisms were observed. While phosphonium salts had a cytostatic effect, blocking cell division, guanidines exhibited apoptotic pathway leading to cell death.

Therefore, conjugation of coumarin and lipophilic cations constitutes an attractive and innovative design for developing new chemotherapeutic agents in future.

4. Experimental section

4.1. Materials and methods

4.1.1. General procedures

The conditions reported previously [61] for TLC monitoring, column chromatography purifications, and NMR and HRMS spectra were used herein.

4.1.2. Carbonic anhydrases inhibition

Inhibition assessments of carbonic anhydrases were accomplished using the stopped-flow CO₂ hydrase assay [33]. hCAs I, II, IX, XI used herein are recombinant and tested in a 5–12 nM range.

4.1.3. Molecular modelling analysis

See Supporting Information (S3).

4.1.4. Antiproliferative activities

See Supporting Information (S4).

4.1.5. Sulforhodamine B assay

See Supporting Information (S5).

4.1.6. Cell death analysis

See Supporting Information (S6).

4.1.7. TMRE assay

See Supporting Information (S6).

4.1.8. Live cell imaging

Minor modifications on the original procedure reported by some of us were conducted [62]. Conditions are described in the Supporting Information section (S7).

4.2. Chemistry

4.2.1. General procedure for the preparation of coumarins 3a-d

See Supporting information (S8).

4.2.2. General procedure for the preparation of 7-O-alkylated coumarins 4a-g

See Supporting Information (S8).

4.2.3. General procedure for the preparation of triphenylphosphonium salts 5b-g

See Supporting Information (S8). Full characterization of compounds 5b-f can be found in Supporting Information (S8-S10).

4.3.2.6. {5-[(3'-Chloro-4'-methyl-2'-oxo-2'H-chromen-7-yl)oxy]pentyl} triphenylphosphonium bromide (5g). Bromoderivative 4 g (50 mg, 0.14 mmol) and PPh₃ (182.3 mg, 0.70 mmol) were used. Column chromatography afforded 5g as a brown foam. Yield: 87.1 mg, quant.; R_f 0.23 (20:1 CH₂Cl₂-MeOH); ¹H NMR (300 MHz, CDCl₃) δ 7.78 (m, 9H, Ph), 7.65 (m, 6H, Ph), 7.45 (d, 1H, $J_{5',6'}$ = 8.9 Hz, H-5'), 6.80 (dd, 1H, $J_{6',5'}$ = 8.9 Hz, $J_{6',8'}$ = 2.3 Hz, H-6'), 6.58 (d, 1H, $J_{8',6'}$ = 2.3 Hz, H-8'), 3.91 (m, 2H, CH₂O), 3.72 (m, 2H, CH₂P), 2.46 (s, 3H, CH₃), 1.78 (m, 6H, 3CH₂) ppm; ¹³C NMR (75.5 MHz, CDCl₃) δ 161.7 (C-7'), 157.3 (C-2'), 152.7 (C-9'), 148.1 (C-4'), 135.0 (d, $^4J_{C,P}$ = 2.9 Hz, Ar-Cp), 133.5 (d, $^2J_{C,P}$ = 10.0 Hz, Ar-o), 130.4 (d, $^3J_{C,P}$ = 12.5 Hz, Ar-Cm), 125.9 (C-5'), 118.0 (d, $^1J_{C,P}$ = 86.0 Hz, Ar-Cipso), 117.2 (C-3'), 112.9 (C-10'), 112.8 (C-6'), 101.3 (C-8'), 68.1 (CH₂O), 28.2 (CH₂CH₂O), 26.8 (d, $^1J_{C,P}$ = 16.6 Hz, CH₂P), 22.9 (CH₂), 22.3 (d, $^2J_{C,P}$ = 4.4 Hz, CH₂CH₂P), 16.1 (CH₃), 12.9 (CH₃) ppm; HRESI-MS *m/z* calcd. for C₃₃H₃₁ClO₃P⁺ ([M-Br]⁺): 541.1694, found: 541.1692.

4.2.4. General procedure for the preparation of amino-coumarins 9a,c-g

See Supporting Information (S10).

4.2.5. General procedure for the preparation of coumarin-derived thioureas 10a,c-g

See Supporting Information (S12). Full characterization of compounds 10a, 10c-g can be found therein.

4.2.6. General procedure for the preparation of coumarin-derived guanidines 14a,c-g

See Supporting Information (S15). Full characterization of compounds 14a,14d-g can be found therein.

4.2.6.1. Nⁿ-Benzyl-N-{5-[(4'-methyl-2'-oxo-2'H-chromen-7-yl)oxy]pentyl}-N-(p-tolyl)guanidine (14c).

Thiourea 10c (31 mg, 75 μ mol), BnNH₂ (42

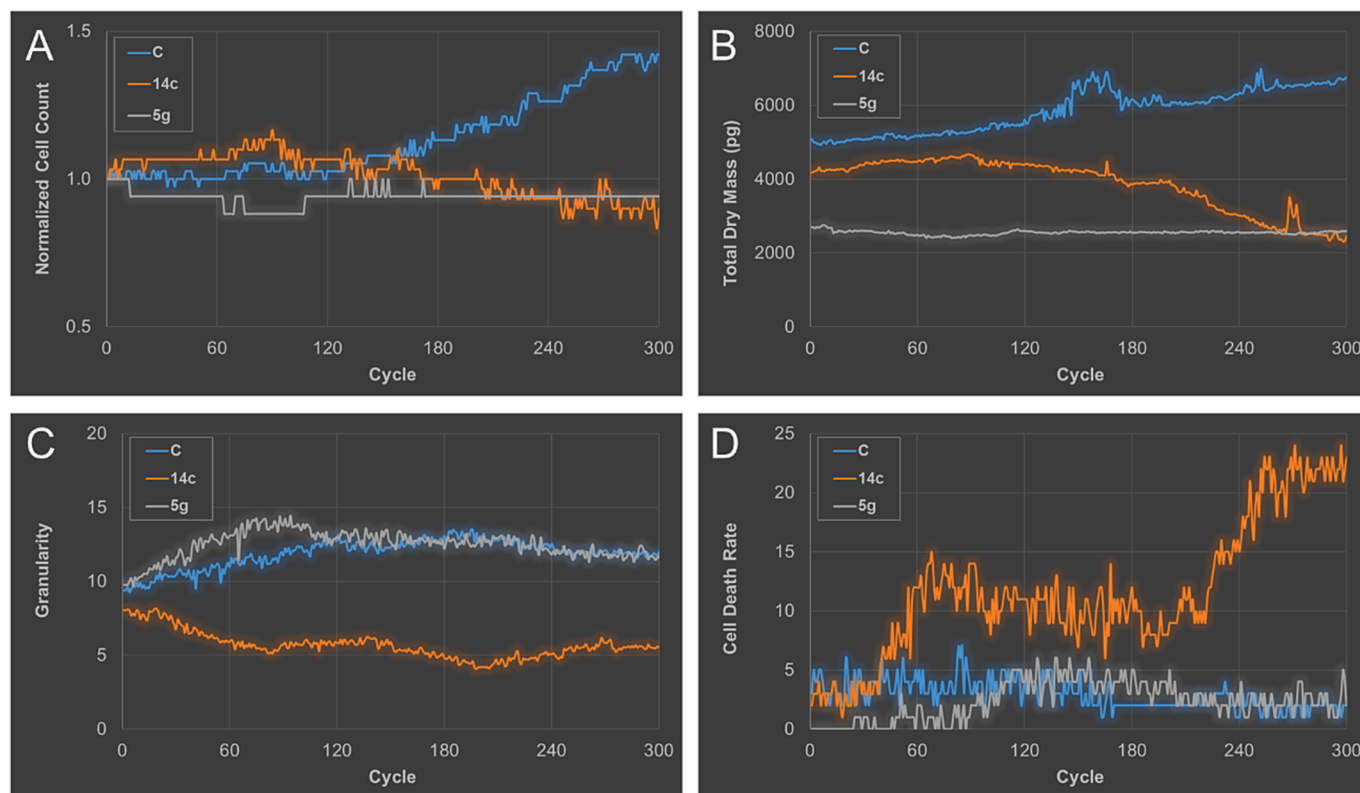


Fig. 8. Kinetics of phenotypic parameters for SW1573 cells exposed to compounds **5g** (3 μ M) and **14c** (21 μ M) for 15 h, in comparison with untreated cells or control (C, blue line). (For interpretation of the references to colour in this figure legend, the reader is referred to the web version of this article.)

μ L, 0.38 mmol) and yellow HgO (65.0 mg, 0.30 mmol) were used. Column chromatography afforded **14c** as a brown oil. Yield: 30.5 mg (84 %). R_f 0.15 (5:1 CH_2Cl_2 -MeOH); ^1H NMR (300 MHz, CDCl_3) δ 7.39 (d, 1H, $J_{5,6} = 8.8$ Hz, H-5), 7.28–7.14 (m, 5H, Ar-H, Ph), 6.99 (m, 2H, Ar-Ho), 6.75 (m, 3H, H-6, Ar-Hm), 6.68 (d, 1H, $J_{8,9} = 2.4$ Hz, H-8), 6.03 (q, 1H, $J_{3,\text{CH}_3} = 1.1$ Hz, H-3), 4.29 (s, 2H, CH_2Ph), 3.87 (t, 2H, $J_{\text{H,H}} = 6.3$ Hz, CH_2O), 3.11 (t, 2H, $J_{\text{H,H}} = 6.9$ Hz, CH_2N), 2.31 (d, 3H, $J_{\text{CH}_3,3} = 1.1$ Hz, CH_3), 2.30 (s, 3H, CH_3 -Ar), 1.69 (m, 2H, CH_2), 1.47 (m, 2H, CH_2), 1.32 (m, 2H, CH_2) ppm; ^{13}C NMR (75.5 MHz, CDCl_3) δ 162.0 (C-7), 161.3 (C-2), 155.2 (C-9), 152.3 (C-4), 151.8 (C=N), 145.48 (Ar-Cipso), 138.7 (Ar-Cipso Ph), 131.5 (Ar-Cp), 129.9 (Ar-Co), 128.7 (Ar-Co Ph), 127.5 (Ar-Cp Ph), 127.2 (Ar-Cm Ph), 125.5 (C-5), 123.3 (Ar-Cm), 113.4 (C-10), 112.5 (C-6), 111.7 (C-3), 101.2 (C-8), 68.2 (CH_2O), 46.0 (CH_2Ph), 41.8 (CH_2N), 29.3 ($\text{CH}_2\text{CH}_2\text{O}$), 28.5 ($\text{CH}_2\text{CH}_2\text{N}$), 23.2 (CH_2), 20.7 (Ar- CH_3), 18.6 (CH_3) ppm; HRESI-MS m/z calcd. for $\text{C}_{30}\text{H}_{34}\text{N}_3\text{O}_3$ ($[\text{M} + \text{H}]^+$): 484.2595, found: 484.2591.

CRedit authorship contribution statement. **Alma Fuentes-Aguilar:** Methodology, Investigation. **Aday González-Bakker:** Methodology, Investigation, Data curation. **Mirna Jovanović:** Methodology, Investigation, Formal analysis, Data curation. **Sofija Jovanović Stojanov:** Methodology, Investigation, Formal analysis, Data curation. **Adrián Puerta:** Methodology, Investigation, Formal analysis, Data curation. **Adriana Gargano:** Methodology, Investigation, Formal analysis, Data curation. **Jelena Dinić:** Writing – review & editing, Supervision, Methodology, Investigation, Formal analysis, Conceptualization. **José L. Vega-Báez:** Writing – review & editing, Supervision, Formal analysis. **Penélope Merino-Montiel:** Writing – review & editing, Supervision, Formal analysis. **Sara Montiel-Smith:** Writing – review & editing, Formal analysis. **Stefano Alcaro:** Writing – review & editing, Supervision, Methodology, Formal analysis, Data curation. **Alessio Nocentini:** Writing – review & editing, Methodology, Investigation, Formal analysis, Data curation. **Milica Pešić:** Writing – review & editing,

Methodology, Investigation, Funding acquisition, Formal analysis, Conceptualization. **Claudiu T. Supuran:** Writing – review & editing, Methodology, Investigation, Formal analysis, Conceptualization. **José M. Padrón:** Writing – review & editing, Supervision, Formal analysis. **José G. Fernández-Bolaños:** Writing – review & editing, Supervision, Formal analysis. **Óscar López:** Writing – review & editing, Writing – original draft, Supervision, Methodology, Funding acquisition, Conceptualization.

Declaration of competing interest

The authors declare that they have no known competing financial interests or personal relationships that could have appeared to influence the work reported in this paper.

Acknowledgements

J.G.F.-B. and Ó.L. thank Grant PID2020-116460RB-I00 funded by MCIN/AEI/10.13039/501100011033, and Junta de Andalucía (FQM134) for financial support. A.F.-A. thanks the CONACYT (Mexico) for the award of a fellowship. A.G.-B., A.P. and J.M.P. thank the Spanish Government (Project PID2021-123059OB-I00 funded by MCIN/AEI/10.13039/501100011033 / FEDER, UE) for financial support. A.P. thanks the EU Social Fund (FSE) and the Canary Islands ACIISI for a predoctoral grant TESIS2020010055. A.G.-B. thanks the Asociación Española Contra el Cáncer (AECC) de Santa Cruz de Tenerife for predoctoral grant PRDTF233958GONZ. M.J., J.D., S.J.S. and M.P. thank the Ministry of science, technological development and innovation of the Republic of Serbia for financial support (451-03-47/2023-01/200007). This work was performed within the framework of COST Action CA17104 STRATAGEM “New diagnostic and therapeutic tools against multidrug resistant tumors”. We would also like to thank the Servicio de Resonancia Magnética Nuclear, CITIUS (University of Seville) for the

performance of NMR experiments.

Appendix A. Supplementary data

General procedures for molecular modelling, biological assays and chemical synthesis; full characterization of new compounds **5b-f**, **10a**, **10c-g**, **11**, **14a**, **14d-g**; Table S1 (G-score for approved CA inhibitors); Tables S2 and S3 (total interactions predicted between **5c,f,g**, **14c** and CA XII and IX, respectively); Video S1: Live-cell imaging control experiment (non-treated SW1573 cells); Video S2: Live-cell imaging experiment of SW1573 cells treated with **5g** (3 μ M); Video S3: Live-cell imaging experiment of SW1573 cells treated with **14c** (21 μ M); 1 H- and 13 C-NMR spectra of new compounds. Supplementary data to this article can be found online at <https://doi.org/10.1016/j.bioorg.2024.107168>.

References

- [1] A. Franconetti, Ó. López, J.G. Fernández-Bolaños, Carbohydrates: potential sweet tools against cancer, *Curr. Med. Chem.* 27 (2020) 1206–1242.
- [2] A. Jassim, E.P. Rahrmann, B.D. Simons, R.J. Gilbertson, Cancers make their own luck: theories of cancer origins, *Nat. Rev. Cancer* (2023) 710–724.
- [3] C. Pucci, C. Martinelli, G. Ciofani, Innovative approaches for cancer treatment: current perspectives and new challenges, *ecancer* 13 (2019) 961.
- [4] L. Racca, V. Cauda, Remotely activated nanoparticles for anticancer therapy, *Nano-Micro Lett.* 13 (2021) 11.
- [5] M. Wu, M. Wang, H. Jia, P. Wu, Extracellular vesicles: emerging anti-cancer drugs and advanced functionalization platforms for cancer therapy, *Drug Deliv.* 29 (2022) 2513–2538.
- [6] A.J. Kerr, D. Dodwell, P. McGale, F. Holt, F. Duane, G. Mannu, S.C. Darby, C. W. Taylor, Adjuvant and neoadjuvant breast cancer treatments: A systematic review of their effects on mortality, *Cancer Treat. Rev.* 105 (2022) 102375.
- [7] Z. Zhou, M. Li, Targeted therapies for cancer, *BMC Med.* 20 (2022) 90.
- [8] E.B. Yahya, A.M. Alqadhi, Recent trends in cancer therapy: A review on the current state of gene delivery, *Life Sci.* 269 (2021) 119087.
- [9] T. Kaur, D. Sharma, Expansion of thermometry in magnetic hyperthermia cancer therapy: antecedence and aftermath, *Nanomedicine* 17 (2022) 1607–1623.
- [10] S.J. Chen, S.C. Wang, Y.C. Chen, The immunotherapy for colorectal cancer, lung cancer and pancreatic cancer, *Int. J. Mol. Sci.* 22 (2021) 12836.
- [11] J. Liu, M. Fu, M. Wang, D. Wan, Y. Wei, X. Wei, Cancer vaccines as promising immuno-therapeutics: platforms and current progress, *J. Hematol. Oncol.* 15 (2022) 28.
- [12] S. Jin, Y. Sun, X. Liang, X. Gu, J. Ning, Y. Xu, S. Chen, Emerging new therapeutic antibody derivatives for cancer treatment, *Signal Transduct. Target. Ther.* 7 (2022) 39.
- [13] K. Nurgali, J.A. Rudd, H. Was, R. Abalo, Cancer therapy: The challenge of handling a double-edged sword, *Front. Pharmacol.* 13 (2022) 1007762.
- [14] A. Valente, A. Podolski-Renić, I. Poetsch, N. Filipović, Ó. López, I. Turel, P. Heffeter, Metal- and metalloid-based compounds to target and reverse cancer multidrug resistance, *Drug Resist. Updat.* 58 (2021) 100778.
- [15] Focusing on mitochondrial form and function, *Nat Cell Biol.* 20 (2018) 735.
- [16] M. Xia, Y. Zhang, K. Jin, Z. Lu, Z. Zeng, W. Xiong, Communication between mitochondria and other organelles: a brand-new perspective on mitochondria in cancer, *Cell Biosci.* 9 (2019) 27.
- [17] M.P. Murphy, R.C. Hartley, Mitochondria as a therapeutic target for common pathologies, *Nat. Rev. Drug Discov.* 17 (2018) 865–886.
- [18] D. Guzmán-Villanueva, V. Weissig, Mitochondria-targeted agents: mitochondriotropics, mitochondriotoxics, and Mitocans, in: H. Singh, S.S. Sheu (Eds.), *Pharmacology of Mitochondria. Handbook of Experimental Pharmacology*, vol. 240, Springer, Cham, 2016, pp. 423–438.
- [19] L. Dong, V. Gopalan, O. Holland, J. Neuzil, Mitocans revisited: mitochondrial targeting as efficient anti-cancer therapy, *Int. J. Mol. Sci.* 21 (2020) 7941.
- [20] J. Zielonka, A. Sikora, M. Hardy, O. Ouari, J. Vasquez-Vivar, G. Cheng, M. López, B. Kalyanaraman, Mitochondria-targeted triphenylphosphonium-based compounds: syntheses, mechanisms of action, and therapeutic and diagnostic applications, *Chem. Rev.* 117 (2017) 10043–10120.
- [21] J.S. Modica-Napolitano, J.R. Aprile, Delocalized lipophilic cations selectively target the mitochondria of carcinoma cells, *Adv. Drug Deliv. Rev.* 49 (2001) 63–70.
- [22] C.T. Supuran, A simple yet multifaceted 90 years old, evergreen enzyme: Carbonic anhydrase, its inhibition and activation, *Bioorg. Med. Chem. Lett.* 93 (2023) 129411.
- [23] A. Nocentini, C.T. Supuran, C. Capasso, An overview on the recently discovered iota-carbonic anhydrases, *J. Enzyme Inhib. Med. Chem.* 36 (2021) 1988–1995.
- [24] A. Nocentini, W.A. Donald, C.T. Supuran, in: C.T. Supuran, A. Nocentini (Eds.), *Carbonic Anhydrases-Biochemistry and Pharmacology of an Evergreen Pharmaceutical Target*, Academic Press, 2019, pp. 151–185.
- [25] C.T. Supuran, Carbonic anhydrases: novel therapeutic applications for inhibitors and activators, *Nat. Rev. Drug. Discov.* 7 (2008) 168–181.
- [26] A. Aspatwar, M.E.E. Tolvanen, S. Parkkila, An update on carbonic anhydrase-related proteins VIII, X and XI, *J. Enzyme Inhib. Med. Chem.* 28 (2013) 1129–1142.
- [27] C.T. Supuran, A.S.A. Altamimi, F. Carta, Carbonic anhydrase inhibition and the management of glaucoma: a literature and patent review 2013–2019, *Expert Opin. Ther. Pat.* 29 (2019) 781–792.
- [28] C.T. Supuran, C. Capasso, Antibacterial carbonic anhydrase inhibitors: an update on the recent literature, *Expert Opin. Ther. Pat.* 30 (2020) 963–982.
- [29] C.T. Supuran, Anti-obesity carbonic anhydrase inhibitors: challenges and opportunities, *J. Enzyme Inhib. Med. Chem.* 37 (2022) 2478–2488.
- [30] C.T. Supuran, Targeting carbonic anhydrases for the management of hypoxic metastatic tumors, *Expert Opin. Ther. Pat.* 33 (2023) 701–720.
- [31] G. Provensi, F. Carta, A. Nocentini, C.T. Supuran, F. Casamenti, M.B. Passani, S. Fossati, A new kid on the block? Carbonic anhydrases as possible new targets in Alzheimer's disease, *Int. J. Mol. Sci.* 20 (2019) 4724.
- [32] A. Fuentes-Aguilar, P. Merino-Montiel, S. Montiel-Smith, S. Meza-Reyes, J.L. Vega-Báez, A. Puerta, M.X. Fernandes, J.M. Padrón, A. Petreni, A. Nocentini, C. T. Supuran, Ó. López, J.G. Fernández-Bolaños, 2-Aminobenzoxazole-appended coumarins as potent and selective inhibitors of tumour-associated carbonic anhydrases, *J. Enzyme Inhib. Med. Chem.* 37 (2022) 168–177.
- [33] G. Arrighi, A. Puerta, A. Petreni, F.J. Hicke, A. Nocentini, M.X. Fernandes, J. M. Padrón, C.T. Supuran, J.G. Fernández-Bolaños, Ó. López, Squaramide-tethered sulfonamides and coumarins: synthesis, inhibition of tumor-associated CAs IX and XII and docking simulations, *Int. J. Mol. Sci.* 23 (2022) 7685.
- [34] A.S. Zambare, F.A.K. Khan, S.P. Zambare, S.D. Shinde, J.N. Sangshetti, Recent advances in the synthesis of coumarin derivatives via Pechmann condensation, *Curr. Org. Chem.* 20 (2016) 798–828.
- [35] B.G. Lake, J.G. Evans, D.F.V. Lewis, R.J. Price, Studies on the acute effects of coumarin and some coumarin derivatives in the rat, *Food Chem. Toxicol.* 32 (1994) 357–363.
- [36] V.K. Yadav, V.P. Srivastava, L. Dhar, S. Yadav, Iodide catalyzed synthesis of 2-aminobenzoxazoles via oxidative cyclodesulfurization of phenolic thioureas with hydrogen peroxide, *Tetrahedron Lett.* 59 (2018) 252–255.
- [37] I. Maya, Ó. López, S. Maza, J.G. Fernández-Bolaños, J. Fuentes, A facile access to ureido sugars. Synthesis of urea-bridged β -cyclodextrins, *Tetrahedron Lett.* 44 (2003) 8539–8543.
- [38] Ó. López, I. Maya, V. Ulgar, I. Robina, J. Fuentes, J.G. Fernández-Bolaños, Expeditious synthesis of cyclic isourea derivatives of β -D-glucopyranosylamine, *Tetrahedron Lett.* 43 (2002) 4313–4316.
- [39] Ó. López, I. Maya, J. Fuentes, J.G. Fernández-Bolaños, Simple and efficient synthesis of O-unprotected glycosyl thiourea and isourea derivatives from glycosylamines, *Tetrahedron* 60 (2004) 61–72.
- [40] L.L. Romero-Hernández, P. Merino-Montiel, S. Meza-Reyes, J.L. Vega-Báez, Ó. López, J.M. Padrón, S. Montiel-Smith, Synthesis of unprecedented steroidal spiro heterocycles as potential antiproliferative drugs, *Eur. J. Med. Chem.* 143 (2018) 21–32.
- [41] J.M. Márquez, Ó. López, I. Maya, J. Fuentes, J.G. Fernández-Bolaños, Taurine isothiocyanate: a versatile intermediate for the preparation of ureas, thioureas, and guanidines. Taurine-derived cyclodextrins, *Tetrahedron Lett.* 49 (2008) 3912–3915.
- [42] V.P. Taori, H. Lu, T.M. Reineke, Structure-activity examination of poly (glycoamidoguanidine)s: glycopolycations containing guanidine units for nucleic acid delivery, *Biomacromolecules* 12 (2011) 2055–2063.
- [43] W. Liu, Q. Li, F. Cheng, D. Shi, Z. Cao, Synthesis of novel glycosyl 1,3,4-oxadiazole derivatives, *Heterocycl. Commun.* 20 (2014) 333–338.
- [44] A. Maresca, C. Temperini, H. Vu, N.B. Pham, S.A. Poulsen, A. Scozzafava, R. J. Quinn, C.T. Supuran, Non-zinc mediated inhibition of carbonic anhydrases: coumarins are a new class of suicide inhibitors, *J. Am. Chem. Soc.* 131 (2009) 3057–3062.
- [45] Schrödinger. Maestro Graphics User Interface; Schrödinger LLC.: New York, NY, USA, 2018.
- [46] M. Pestic, J.Z. Markovic, D. Jankovic, S. Kanazir, I.D. Markovic, L. Rakic, S. Ruzdžic, Induced resistance in the human non small cell lung carcinoma (NCI-H460) cell line in vitro by anticancer drugs, *J. Chemother.* 18 (2006) 66–73.
- [47] A. Podolski-Renić, T. Anđelković, J. Banković, N. Tanić, S. Ruzdžic, M. Pestic, The role of paclitaxel in the development and treatment of multidrug resistant cancer cell lines, *Biomed. Pharmacother.* 65 (2011) 345–353.
- [48] E. Teodori, L. Braconi, S. Bua, A. Lapucci, G. Bartolucci, D. Manetti, M. N. Romanelli, S. Dei, C.T. Supuran, M. Coronnello, Dual P-glycoprotein and CA XII inhibitors: a new strategy to reverse the P-gp mediated multidrug resistance (MDR) in cancer cells, *Molecules* 25 (2020) 1748.
- [49] B. von Neubeck, G. Gondi, C. Riganti, C. Pan, A. Parra Damas, H. Scherb, A. Ertürk, R. Zeidler, An inhibitory antibody targeting carbonic anhydrase XII abrogates chemoresistance and significantly reduces lung metastases in an orthotopic breast cancer model in vivo, *J. Cancer* 143 (2018) 2065–2075.
- [50] A. Podolski-Renić, J. Dinic, T. Stankovic, M. Jovanovic, A. Ramovic, A. Pustenko, R. Zalubovskis, M. Pestic, Sulfocoumarins, specific carbonic anhydrase IX and XII inhibitors, interact with cancer multidrug resistant phenotype through pH regulation and reverse P-glycoprotein mediated resistance, *Eur. J. Pharm. Sci.* 138 (2019) 105012.
- [51] K.F. Tonissen, S.A. Poulsen, Carbonic anhydrase XII inhibition overcomes P-glycoprotein-mediated drug resistance: a potential new combination therapy in cancer, *Cancer Drug Resist.* 4 (2021) 343–355.
- [52] K.M. Bailey, J.W. Wojtkowiak, A.I. Hashim, R.J. Gillies, Targeting the metabolic microenvironment of tumors, *Adv. Pharmacol.* 65 (2012) 63–107.
- [53] Y.G. Lee, D.H. Park, Y.C. Chae, Role of mitochondrial stress response in cancer progression, *Cells* 11 (2022) 771.
- [54] G.L. Semenza, Hypoxia-inducible factors: mediators of cancer progression and targets for cancer therapy, *Trends Pharmacol. Sci.* 33 (2012) 207–214.

- [55] S. Ivanov, S.Y. Liao, A. Ivanova, A. Danilkovitch-Miagkova, N. Tarasova, G. Weirich, M.J. Merrill, M.A. Proescholdt, E.H. Oldfield, J. Lee, J. Zavada, A. Waheed, W. Sly, M.I. Lerman, E.J. Stanbridge, Expression of hypoxia-inducible cell-surface transmembrane carbonic anhydrases in human cancer, *Am. J. Pathol.* 158 (2001) 905–919.
- [56] Z. Chen, L. Ai, M.Y. Mboge, C. Tu, R. McKenna, K.D. Brown, C.D. Heldermon, S. C. Frost, Differential expression and function of CAIX and CAXII in breast cancer: A comparison between tumorgraft models and cells, *PLoS One* 13 (2018) e0199476.
- [57] O. Sedlakova, E. Svastova, M. Takacova, J. Kopacek, J. Pastorek, S. Pastorekova, Carbonic anhydrase IX, a hypoxia-induced catalytic component of the pH regulating machinery in tumors, *Front. Physiol.* 4 (2014) 400.
- [58] T. Wang, D. Eskandari, D. Zou, L. Grote, J. Hedner, Increased carbonic anhydrase activity is associated with sleep apnea severity and related hypoxemia, *Sleep* 38 (2015) 1067–1073.
- [59] H. Thomas, H.M. Coley, Overcoming multidrug resistance in cancer: an update on the clinical strategy of inhibiting p-glycoprotein, *Cancer Control* 10 (2003) 159–165.
- [60] S. Salucci, M. Battistelli, S. Burattini, F. Sbrana, E. Falcieri, Holotomographic microscopy: a new approach to detect apoptotic cell features, *Microsc. Res. Tech.* 83 (2020) 1464–1470.
- [61] F.J. Hicke, A. Puerta, J. Dinić, M. Pešić, J.M. Padrón, Ó. López, J.G. Fernández-Bolaños, Straightforward access to novel mitochondriotropics derived from 2-arylethanol as potent and selective antiproliferative agents, *Eur. J. Med. Chem.* 228 (2022) 113980.
- [62] M.C. Padilla-Pérez, M. Elena, A. Sánchez-Fernandez, A. Gonzalez-Bakker, J. M. Puerta, F. Padrón, A.I. Martín-Loro, J.M.G. Arroba, J.M. García Fernández, C. Ortiz Mellet, Fluoro-labelled sp²-iminoglycolipids with immunomodulatory properties, *Eur. J. Med. Chem.* 255 (2023) 115930.